
Kuru E, Lambert C, Rittichier J, Till R, Ducret A, Derouaux A, Gray J, Biboy J, Vollmer W, VanNieuwenhze M, Brun YV, Sockett RE. [Fluorescent D-amino-acids reveal bi-cellular cell wall modifications important for *Bdellovibrio bacteriovorus* predation](#). *Nature Microbiology* 2017, **2**, 1648-1657.

DOI link

<https://doi.org/10.1038/s41564-017-0029-y>

ePrints link

<http://eprint.ncl.ac.uk/239009>

Date deposited

12/12/2017

Embargo release date

03/04/2018

Copyright

This is the authors' accepted manuscript of an article that has been published in its final definitive form by Nature Publishing Group, 2017

**Fluorescent D-amino-acids reveal bi-cellular cell wall modifications important for
Bdellovibrio bacteriovorus predation**

Erkin Kuru^{1,5}†, Carey Lambert²†, Jonathan Rittichier^{3,5}, Rob Till², Adrien Ducret^{1,6}, Adeline Derouaux^{4,7}, Waldemar Vollmer⁴, Michael Van Nieuwenhze³, Yves V. Brun¹ and R. Elizabeth Sockett^{2*}

†These authors contributed equally.

*Corresponding Author

¹Department of Biology, Indiana University Bloomington, Bloomington, IN 47405,
USA

²School of Life Sciences, Nottingham University, Queen's Medical Centre, Nottingham NG7
2UH, UK.

³Department of Chemistry, Indiana University Bloomington, Bloomington, IN 47405,
USA

⁴The Centre for Bacterial Cell Biology, Baddiley Clark Building, Medical School, Newcastle
University, Richardson Road, Newcastle upon Tyne, NE2 4AX, UK

⁵Current address: Department of Genetics, Harvard Medical School, Boston, MA 02115, USA

⁶Bases Moléculaires et Structurales des Systèmes Infectieux, IBCP, Université Lyon 1, CNRS,
UMR 5086, 7 passage du Vercors, 69367 Lyon Cedex 07, France

⁷Current address: Xpress Biologics, Tour GIGA B34 (+3), Avenue de l'Hôpital, 11, B-4000
Liège (Sart-Tilman), Belgique

Modification of essential bacterial peptidoglycan (PG) containing cell walls can lead to antibiotic resistance, for example β -lactam resistance by L,D-transpeptidase activities. Predatory *Bdellovibrio bacteriovorus* are naturally antibacterial and combat infections by traversing, modifying and finally destroying walls of Gram-negative prey bacteria, modifying their own PG as they grow inside prey. Historically, these multi-enzymatic processes on two similar PG walls have proved challenging to elucidate. Here, with a new PG labelling approach utilizing timed pulses of multiple fluorescent D-amino acids (FDAAs), we illuminate dynamic changes that predator and prey walls go through during the different phases of bacteria:bacteria invasion. We show formation of a reinforced circular port-hole in the prey wall; L,D-transpeptidase_{Bd} mediated D-amino acid modifications strengthening prey PG during *Bdellovibrio* invasion and a zonal mode of elongation. This process is followed by unconventional, multi-point and synchronous septation of the intracellular *Bdellovibrio*, accommodating odd- and even-numbered progeny formation by non-binary division.

Article

Peptidoglycan (PG) is a shape-determining, essential macromolecule common to the bacterial domain. The mature PG wall of bacteria is made by glycan polymerization and peptide crosslinking of a D-amino acid-rich muramyl pentapeptide subunit (**Figure 1a**). This has a relatively conserved peptide sequence of L-Ala, D-Glu, a diamino acid, such as meso-diaminopimelic acid (m-DAP) in Gram-negative bacteria, and almost universally two D-alanine moieties that serve as the 'energy source' for driving PG cross-links in the ATP-less periplasm (**Figure 1a**)¹. These crosslinks give the PG wall its essential load-bearing properties against the bacterial cell's turgor pressure and are made in two basic ways; either 3-4 crosslinks catalysed by normally essential and common Penicillin Binding Proteins (PBP) or 3-3 crosslinks catalysed by normally disposable, variable, L,D-transpeptidases (Ldt) (**Figure 1b**)².

Although PBPs and Ldts are evolutionarily and structurally distinct transpeptidases, research in diverse bacteria showed that both enzyme types can exchange a range of naturally occurring D-amino acids (DAAs) with the 5th and 4th position D-alanines in the peptide stems of PG subunits, respectively³⁻⁵ (**Figure 1b**). Such exchanges are associated with changes in a variety of biophysical properties of the wall^{6,7}, in particular the strength (as determined by osmolarity challenge^{3,8}) in some bacteria. Substrate promiscuity of these transpeptidases toward a diverse set of DAAs⁹ has allowed the development of fluorescent D-amino acids (FDAAs) and their implementation as a means to visualize PG dynamics *in situ*¹⁰⁻¹³

PBP- vs. Ldt- facilitated self-modification of bacterial PG-containing cell walls is not limited to D-amino acid incorporation, however, and is implicated in novel modes of antibiotic resistance. For example, pathogenic Gram-positive bacteria such as *Mycobacterium tuberculosis* or Enterococci bypass β -lactam inhibition of PBP-mediated 3-4 crosslinks by upregulating Ldt-mediated 3-3 crosslinks^{2,6}. On the other hand, although Ldts have a more pronounced presence in Gram-negative bacteria (e.g. 6 homologues in *E. coli*¹⁴) with additional PG-Lipoprotein attachment functions¹⁵, they are not essential^{14,15} and no link between their activities and human health is known. With 19 genes encoding predicted Ldts (Thomas Lerner Ph.D. Thesis, University of Nottingham and Andrew Lovering University of Birmingham, pers comm), we postulated that the Gram-negative predatory *Bdellovibrio bacteriovorus* might be an exception and may use Ldts in PG modifications for their proven predatory pathogen killing action¹⁶

Bdellovibrio bacteriovorus (approximately 1.0 x 0.3 μ m) prey upon (larger) Gram-negative bacterial species by breaching the prey outer-membrane, residing in the modified prey periplasm (forming the “bdelloplast”), resealing and growing within^{17,18}, before finally bursting out to invade more prey (**Figure 1c**). The prey are killed some 20 minutes into predation when electron transport ceases as predator molecules pass across the prey inner membrane¹⁹, however the prey bdelloplast is kept intact for 4 hours to allow “private dining” and consumption of prey contents by the predator. Early electron microscopic work^{20,21} led to the

assumptions that the invading *B. bacteriovorus* would squeeze through the outer layers of the prey bacterium, degrading some type of entry pore in the prey PG containing cell wall, re-sealing this, and modifying the rest of the prey PG. However, as the biochemically similar walls were obscured at the points of contact between the two bacterial cells, this bi-cellular multi-enzymatic process has, until now, been difficult to analyse. Therefore, other than recent work showing the mechanisms of prey cell rounding²⁰, self-protection from auto-rounding^{22,23} and marking of the wall for later destruction²⁴ *B. bacteriovorus* wall-invasion dynamics and enzymology has remained a subject of conjecture.

Here, we combine three differently coloured FDAAs¹⁰ in a series (**Figure 1d-e**) to illuminate the dynamic PG modifications during bacterial predation, simultaneously in two bacterial species. Differential initial FDAAs labelling of prey and predator, and the use of a third FDAAs pulse to probe prey wall modifications by the *B. bacteriovorus* predatory enzymes allowed elucidation of dynamic changes during prey-invasion. 3D- Structured Illumination Microscopy (3D-SIM), resolved the *B. bacteriovorus* processes of :- i) breaching the prey PG, ii) constructing a reinforced porthole in the prey cell wall, iii) resealing the porthole after entry, iv) modifying the prey PG with L,D-transpeptidases, and v) eventually achieving filamentous, intra-bacterial zonal cell growth and synchronous, multi-site septation.

Results

Multi-colour FDAAs microscopy reveals prey versus predator cell wall modifications during invasion

In order to monitor modifications at predator and prey interface, and the predator growth patterns in relation to the different stages of invasion, *B. bacteriovorus* cells and stationary phase prey *E. coli* cells were separately pre-labelled with a green FDAAs, BADA and a red FDAAs, TADA, respectively (see methods for emission maxima). Using these cells, a synchronous predatory invasion co-culture (see methods) was established, and this invasive

culture was further pulse-labelled with a blue FDAA, HADA for 10 minutes at key points during the predation process. The cells were then fixed, washed, and imaged (**Figure 1e**).

In such an experiment, we hypothesized that the FDAA pulses with cyan-blue HADA signal- in contrast to BADA pre-labelled *B. bacteriovorus* walls and TADA pre-labelled *E. coli* walls- would illuminate invasion-related changes in sub-cellular features as HADA incorporation into cell walls. These changes could arise either from transpeptidase mediated FDAA-modification of existing PG or through FDAA incorporation into nascent PG during cell growth¹⁰. In *B. bacteriovorus* predation, initially, predator and prey are live on mixing and later (20-30 mins) prey are dead, but their PG can be modified via predator enzymes. Indeed this was seen, and while the relative total cell wall fluorescence of now-dead prey cells (TADA) showed no appreciable change through the invasive process (**Supplementary Figure 1**); both labelling patterns and signal intensities of pulsed HADA fluorescence showed dramatic differences depending on the stage of the invasion.

HADA pulses early in the infection, 15 or 30 minutes post-mixing of predators with prey (i.e. first 5 or 20 min without any probe then a 10 min HADA pulse) resulted in labelling of various sub-cellular features. In particular, intense, localised, focal HADA marks on the prey PG (and a gradient of HADA signal from that focal point) were seen associated with attached *B. bacteriovorus* cells revealing the entry point (elaborated below), of the *B. bacteriovorus* during the earliest predator-prey interaction (**Figure 1f**).

In order to further characterize these sub-cellular features in early predation, we imaged these labelled cells with high resolution 3D Structured Illumination Microscopy (3D-SIM). 3D-SIM resolved most of these focal marks of HADA labelling as annular ring structures (~%25 of all HADA-bright prey cells investigated at earliest predation point, **Figure 2** and **Supplementary Table 1**) having a width (~0.24 μm ; **Supplementary Table 1**) slightly less than that of a *B. bacteriovorus* cell (~ 0.33 μm) at the point of predator invasive cell pole : prey contact. This is consistent with the *B. bacteriovorus* 'squeezing through the entry pore' idea suggested by electron micrographs in earlier work^{20,25,26}. Therefore, these HADA foci likely indicate the

specific modification of the prey cell wall by predator during entry (**Figure 2a**). The ring of HADA modification was on the prey PG rather than the predator as it appeared to be at the point of prey PG with predator on the outside, inside, or partially entering the prey cell (**Supplementary Figure 2 a-c**). Furthermore, rare instances were observed where the predator had detached from the prey (likely due to shearing during washing steps in the labelling procedure) but the HADA foci were still visible, confirming that these foci were indeed on the prey PG (**Supplementary Figure 2-d**).

To establish that the dark channel in the HADA focal mark was indeed an entry pore in the prey PG we needed to detect the reduction of prey-PG material at the HADA channel centre. Using a more outer-membrane permeable *E. coli imp4213* mutant strain as an alternative prey allowed us to label the prey PG uniformly and more completely with otherwise poorly outer-membrane permeable TADA¹⁰. In these cells, dark pores in the TADA signal (arrowheads TADA channel **Figure 3a**) were present, coincident with, and central within, the HADA ring (**Figure 3a** and **Supplementary Table 2**). These results represent a direct observation of *B. bacteriovorus* generating a pore in the prey PG; a process that had previously been only inferred from indirect evidence^{20,26,27}. Furthermore the pore has a built-up ring of FDAAs around it.

Our multiple-colour labelling approach also allowed us to distinguish clear deformations of the prey cell wall at the point where the *B. bacteriovorus* cell had entered (arrowheads, **Figure 2b**, arrowheads HADA channel **Supplementary Figure 3** and **Supplementary Table 1**) clarifying visually previous suggestions that *B. bacteriovorus* enzymatic modifications of prey cell walls may act to soften them^{22,28}.

To investigate dynamic changes in pores after invasion, we analysed (**Supplementary Table 1, Figure 2c** and **Supplementary Figure 2e**), ~400 HADA labelled *E. coli* S17-1 bdelloplasts containing internalised *B. bacteriovorus*. In 87% of these there was a HADA ring similar to the entry pore on bdelloplasts, located at the prey-predator contact point on the prey wall-proximal pole of the internalised *B. bacteriovorus* cells (red arrowheads, **Supplementary**

Figure 2e and **Supplementary Table 1**). In some cases (13% of the 110 analysed) the HADA patches were filled discs (white arrowheads **Figure 2c** and yellow arrowheads **Supplementary Figure 2e**). Such discs were also coincident with dark pores in TADA label of *E. coli imp4213* mutant bdelloplasts (**Figure 3c** and **Supplementary Table 2**) suggesting that they are sealing discs made by internalised *B. bacteriovorus* to close the prey, keeping the bdelloplast intact for predator consumption of contents.

***B. bacteriovorus* establishment inside prey is accompanied by an L,D-transpeptidase-mediated prey wall modification**

As the *B. bacteriovorus* cells enter the prey periplasm, the prey cells become rounded (**Figure 2a**), forming a bdelloplast¹⁷. During this period, the extent of HADA incorporation to the whole rounding wall of the (now dead) prey substantially increased and peaked around 45 min post-mixing, with ~2 to 4 times more HADA signal-intensity (blue line, **Figure 4a**, see methods for details) than the mean HADA labelling at later 2, 3, and 4 hour predation time points.

Previous global transcriptomic work had shown that the predicted *B. bacteriovorus* L,D-transpeptidase (Ldt) genes, *bd0886* and *bd1176*, are transcriptionally upregulated at 30 minutes from the start of predation ~5- and 6-fold, respectively²⁹. These predicted L,D-transpeptidases, therefore, are good candidates for prey wall modification enzymes during bdelloplast establishment. RT-PCR analysis confirmed that the expression of both genes peaked at 15-30 minutes into predation (**Figure 4b**); time points at which HADA incorporation to the prey walls begins (blue line, **Figure 4a**), while a control gene, *dnaK*, was expressed constitutively throughout the predatory cycle. Deletion of both of these *ldt* genes (leaving 17 *ldt_{Bd}* genes intact) resulted in a $\Delta bd0886\Delta bd1176$ predator (named $\Delta 2ldt$) that caused ~2-4 times less prey HADA incorporation activity than the wild type (blue line vs. orange line, **Figure 4a** and representative images in **Figure 4c** vs. **Figure 4d**). This difference was significant ($p < 0.0001$ for each timepoint except 240min, where $p = 0.016$) of the wild-type versus the mutant suggesting that these two *B. bacteriovorus* *ldt* gene products are responsible for the majority of the overall HADA pulse incorporation into prey wall within the 2 hours during the

predation. A C-terminal fusion of mCherry to one of these two Ldts (Bd1176) localized to the prey bdelloplast, suggesting that this transpeptidase was exported from predator to bdelloplast and so was acting on the prey PG (**Supplementary Figure 4**). Some Bd1176-mCherry fluorescence in the *B. bacteriovorus* cells themselves was also observed, but only minor HADA incorporation in the free-swimming attack phase *B. bacteriovorus* themselves suggests that the enzyme has low or no activity inside predators (**Supplementary Figure 4**). Both Bd0886 and Bd1176 are predicted (Signal P 4.0) to have a signal peptide at the N-terminus for sec-dependent secretion, but no other predicted transmembrane domains. This secretion is similar to that for predatory DacB enzymes of *B. bacteriovorus* which have an associated periplasmic immunity protein (Bd3460) protecting the *B. bacteriovorus* self PG from the action of these enzymes^{22,23}.

Bdelloplast wall modification is largely by the action of *B. bacteriovorus* enzymes which act upon uncrosslinked tetrapeptides of the prey PG

In order to test the nature of the bdelloplast wall modification, we quantified HADA incorporation in bdelloplasts formed by *B. bacteriovorus* predation on different *E. coli* prey lacking different PG modification functionalities. The prey strain *E. coli* BW25113 Δ 6LDT lacks all of the 6 *E. coli* L,D-transpeptidases (and therefore any L,D-transpeptidation activity) and should be enriched for tetrapeptides in its PG with unmodified terminal D-alanine residues^{14,15,30}. The prey strain, *E. coli* BW25113 Δ dacA, lacks the major *E. coli* D,D-carboxypeptidase DacA and so should be enriched in pentapeptides in its PG. The prey strain *E. coli* BW25113 Δ 6LDT Δ dacA lacks all 6 L,D-transpeptidases and the D,D-carboxypeptidase DacA and so should be enriched for both pentapeptides and tetrapeptides in its PG. Compared to the wild type prey strain, *E. coli* BW25113 wt, predation of these strains by *B. bacteriovorus* and pulse labelling with HADA at 35-45 minutes post mixing of predator and prey, resulted in significantly more HADA incorporation for both prey strains lacking the L,D-transpeptidase activity (Δ 6LDT and Δ 6LDT Δ dacA, **Figure 5a**), but with no significant difference for prey lacking DacA alone (**Figure 5a**). In the absence of *B. bacteriovorus* predation, prey cells in

Ca/HEPES buffer pulsed with HADA showed a fraction of the HADA incorporation when compared to the prey strains subjected to *B. bacteriovorus* predation (~1.5-14.6% of HADA incorporation, controls versus +Bds, **Figure 5a**). The majority of the *E. coli* self-labelling (in controls in the absence of *B. bacteriovorus* **Figure 5a**) was absent in the *E. coli* BW25113 $\Delta 6LDT$ showing the Ldt_{EC} to be responsible for this small amount of labelling. That predation of this strain actually resulted in more HADA incorporation further supports the notion that this incorporation is by *Bdellovibrio* encoded enzymes rather than those of the prey. Altogether, these results suggest that a significant proportion of the strong HADA incorporation observed on the prey PG during predation involves predator L,D-transpeptidase activity on tetrapeptides of the prey bdelloplast PG (and not D,D-transpeptidase activity on pentapeptides). These data, along with Bd1176-mCherry and $\Delta 2ldt$ data above, show that this activity comes from L,D-transpeptidases secreted by the *B. bacteriovorus* and not due to lingering activities of prey Ldt enzymes.

L,D-Transpeptidase_{Bd} -mediated prey wall modification confers bdelloplast physical robustness

At the commencement of bdelloplast formation, the invaded prey cell is rounded by the action of *B. bacteriovorus* D,D-endopeptidases cutting 3-4 crosslinks in prey PG²². Formation of new 3-3 crosslinks or incorporation of alternative D-amino acids such as m-DAP^{27,31} by *B. bacteriovorus* Ldts at this point could strengthen and/or stabilise the bdelloplast structure. The $\Delta 2ldt$ mutant predator still preyed upon *E. coli* and incorporated a low level of HADA into the prey cell walls (**Figure 4**), suggesting that other predator enzyme activities may also contribute to prey modification. Their role in DAA incorporation, however, suggests that the products of *bd0886* and *bd1176* are important players in prey PG modification. To test this idea further, we assayed the stability of bdelloplasts produced by wild type *B. bacteriovorus* or by $\Delta 2ldt$ mutant predator under osmotic challenge using the β -galactosidase substrate chlorophenyl red- β -D-galactopyranoside (CPRG) method to screen for damage to bacterial cell walls³².

Bdelloplasts, at 1 hour post-synchronous infection of *E. coli* S17-1 (*lac*⁺) prey, when *B. bacteriovorus* are beginning to grow inside prey cells and when Ldt-dependent FDAA transfer has just peaked (**Figure 4a**), were subjected to osmotic upshock or downshock³³. Bdelloplasts were harvested by centrifugation and shocked by resuspension in Ca/HEPES buffer for no shock control- except centrifugation only, Ca/HEPES buffer supplemented with 750mM NaCl (Upshock) or upshock followed by further centrifugation and resuspension in water (Downshock). The buffers for shock and control were supplemented with bacterially impermeant CPRG (20 µg per ml) used to assay for β-galactosidase activity (present by leakage from damaged bdelloplast walls), by spectrophotometry at 574 nm. We observed increased β-galactosidase activity in the supernatant from shocked bdelloplasts formed by Δ*2ldt* mutant predators relative to wild-type in all conditions tested, including a small but significant ($p=0.0084$ by Student's *t*-test) increase in levels from bdelloplasts formed by Δ*2ldt* predators, only subjected to the stress of centrifugation and resuspended in buffer (**Figure 5b**). These data suggest that Bd0886 and Bd1176 L,D-transpeptidase activities strengthen the bdelloplast wall to resist bursting during periods of *B. bacteriovorus* predatory intra-bacterial growth, after prey-entry.

To investigate if this Ldt modification had any effect on the bdelloplast morphology, we measured the sizes and shapes of the prey and bdelloplasts. Early bdelloplasts (45-60 minutes) formed by the Ldt mutant *B. bacteriovorus* were slightly, but significantly ($p<0.0001$) less round than those formed by the wild-type (**Supplementary Figure 5**). We hypothesise that the less robust bdelloplasts formed by the Ldt mutant result in more flexible walls that warped more by the invading *B. bacteriovorus* cell, visible at the earlier stage of invasion after the *B. bacteriovorus* cell squeezed into the full prey cell. At later stages of invasion (2-4 hours) degradation of prey cell content may be why the differences between bdelloplasts formed by the mutant or the wild-type are no longer significant. Differences earlier in the process (15-30 minutes) are more likely to be an artefact of slight asynchrony of infection between the cultures (explanation in **Supplementary Figure 5**).

Multi-coloured FDAA labelling provides direct evidence for the zonal mode of elongation and synchronous division of *B. bacteriovorus* growing inside prey

B. bacteriovorus grow without binary fission, as a single multi-nucleoid filament inside prey³⁴. At later timepoints, after 2 hours post-mixing, we observed filamentous cell elongation of the *B. bacteriovorus* within bdelloplasts (**Figure 6a**)³⁴. Attack phase (AP) *B. bacteriovorus* were added in excess to ensure efficient predation in our experiments and AP predator cells that did not enter prey can be seen to retain substantial initial BADA labelling (**Figures 6a** and yellow arrowheads, **6b**), because they do not replicate outside prey. On the other hand, after 2-3 hour inside prey, we observe some green BADA transfer into the prey bdelloplast structure (BADA signal on bdelloplasts, **Figure 6a**) which may represent a predator-to-prey DAA turnover and transfer event as the growing *B. bacteriovorus* make new PG during elongation. While potentially fascinating, quantifying this inter-wall transfer proved impossible to resolve with current reagents.

3D-SIM imaging showed that *B. bacteriovorus* cells elongate along the filament with numerous, focused zones of growth (labelled with HADA, red arrowheads, **Figure 6b**) covering the entire cell surface except the apparently inert poles (preserving the original BADA signal, green arrowheads, **Figure 6b**). Later, around 3 hours post-mixing, new HADA incorporation appears as defined narrow foci along the filament (**Figure 6a** and red arrowheads **6c**), at points in *B. bacteriovorus* where new division septa would be expected to form synchronously³⁴. After 4 hour post-mixing, these foci become the points of septum formation (**Figure 6a** and yellow arrowheads **6d**). Finally, newly released, attack phase *B. bacteriovorus* daughter cells (white arrowheads, **Figure 6d**) incorporate pulsed HADA all over the cell and can therefore be distinguished from those BADA labelled predators that didn't enter prey cells (excess predators are applied at the start of the experiment) by the presence of a strong HADA fluorescent signal, but low BADA fluorescent signal.

Discussion

Here, using multi coloured FDAA labelling and super-resolution imaging, we directly visualise sub-cellular modifications by *B. bacteriovorus* on *E. coli* PG cell walls and their effects during predation. Our data define an entry port structure by which a *B. bacteriovorus* cell accesses the cytoplasmic membrane face of the prey cell wall and seals itself in. We also show the sites of PG growth in the novel, non-binary fission mode of predator growth. In addition, we show that L,D-transpeptidase enzymes from the *B. bacteriovorus* modify the PG of prey during residency of the predator to establish a stable intracellular niche.

Pioneering enzymology of prey bdelloplast extracts in the 1970s had detected bulk enzyme activities suggestive of extensive predator-modification of prey PG. These included solubilisation of 25% of the *m*-DAP residues on the PG²⁷ and the addition of free *m*-DAP back to the bdelloplast³¹. *m*-DAP is a residue native to PG that has both L- and D- amino acid properties. Therefore, we see FDAAs in our studies acting as visible substrates for these enzymatic, fresco-like changes to the walls of invaded prey caused by *B. bacteriovorus* enzymes. Indeed, we show the *B. bacteriovorus*-facilitated, localised breakdown of the prey wall to form a pore, its re-sealing while also rounding the prey cell wall to form an osmotically stable bdelloplast.

The initial ring of intense FDAA incorporation (with a diameter of 236 nm \pm 28 nm; slightly smaller than the *B. bacteriovorus* cell width) matches with the gap on the prey cell wall at the contact point with the *B. bacteriovorus* pole (**Supplementary Tables 1 and 2, Figures 2a and 3a**) surrounds. Such a re-modelling of the prey PG likely strengthens the predator entry point. Earlier electron microscopy studies had shown circular bleb structures on the attacking *B. bacteriovorus* pole²¹ which could be localised predator secretion machinery used to achieve this pore production. We show also here (**Figures 2c and 3b**) that such entry ports have accumulated centralised FDAA signal after *B. bacteriovorus* entry which might represent a gradual ring-to-disc re-sealing activity of this pore; a process which had previously been only inferred by indirect evidence of “scars” left behind on the prey cell wall at the point of entry³⁵. Determining whether the ring-forming and the re-sealing enzymes are positionally secreted,

soluble enzymes, or membrane bound, allowing such spatially accurate modification; is an interesting question that requires extensive future experimentation.

The most extensive prey cell wall modification occurs 30-45 min after mixing *B. bacteriovorus* with the prey; involving the L,D-transpeptidases with major contributions from 2 of the 19 Ldt_{Bd} enzymes encoded by genes *bd0886* and *bd1176* (**Figure 4a**). These observations may be due to pulsed FDAAs mimicking the incorporation of previously solubilised *m*-DAP reported in early *B. bacteriovorus* studies^{27,31} but this is beyond our present experimentation. Incorporation of non-canonical D-amino acids into the cell wall is a stress response in *Vibrio cholerae*, which is shown to stabilize the PG integrity of the cells in stationary phase³. The incorporation of native *m*-DAP³¹ and/or D-amino acids into the prey cell wall by *B. bacteriovorus* Ldts early in the predation (15 min – 1 hour) could represent an analogous, yet novel means of forming a stabilised and stress resistant bdelloplast. The susceptibility of bdelloplasts formed by the Ldt mutant strain to bursting during osmotic stress (**Figure 5b**) supports this hypothesis. Live bacterial cells have mechanisms to overcome osmotic stresses³², but prey *E. coli* is rapidly killed upon entry of the *B. bacteriovorus*. The predator also extensively modifies the prey cell wall during entry and bdelloplast formation, so a D-amino acid-transfer mechanism for strengthening the bdelloplast could prevent leakage of prey-derived nutrients or even premature lysis (preventing predator replication) in adverse environmental conditions.

FDAAs labelling also elucidated the growth of the intraperiplasmic *B. bacteriovorus* predator directly (**Figure 6**). Growth starts in patches along the length of the *B. bacteriovorus* cell, but not at the poles (**Figure 6a** and **6b**). After *B. bacteriovorus* septation, final predator self PG modification produces attack phase *B. bacteriovorus* (**Figure 6d**) which each emerge with one flagellated and one piliated pole^{25,36}. These experiments provide evidence that both predator poles can carry out bilateral growth, along the length of the cell, rather than one “old” pole remaining attached to the membrane and growth emanating solely from specific regions^{34,37}. Synchronous septum construction (that results in odd or even progeny numbers) is seen along

the length of the filamentous *B. bacteriovorus* growing within the bdelloplast (**Figures 6a, 6c-d**), confirming earlier movies of this novel synchronous division³⁴.

In conclusion, the ability to distinctly label the PG containing cell walls of two different genera of interacting bacteria with different coloured FDAAs, has illuminated a series of dynamic molecular modifications that predatory *B. bacteriovorus* make to prey-cell walls and self-cell walls during their intraperiplasmic lifestyle. These modifications: pore formation and resealing without bacterial bursting and PG remodelling with free small molecules, i.e. DAAs, in dual cell systems are previously uncharacterised in bacteria, and are key mechanisms of predation. Given the inherent promiscuity of virtually all PG containing bacteria to incorporate FDAAs *in situ*^{10,38} we expect this general approach to be helpful for visualising interactions of other complex bacterial communities, e.g. microbiota. Accordingly, we would not be surprised if this and similar approaches illuminate other examples of inter-generic PG modifications with novel functions.

Acknowledgements

We thank Dr Daniel Kearns and his laboratory (Indiana University, USA) for facilities and hospitality to culture *B. bacteriovorus*, Dr Andrew Lovering (University of Birmingham UK) for insights and assistance with the alignment of L,D-transpeptidase protein sequences in *B. bacteriovorus*, Dr Teuta Pilizota (University of Edinburgh UK) for advice on osmotic stress conditions, Dr Rebecca Lowry (University of Nottingham) for assistance in image acquisition, Joe Gray and Jacob Biboy (University of Newcastle) for testing PG preparations. This work was supported by the UK Biotechnology and Biological Sciences Research Council [grant number BB/M010325/1] for CL and by a Leverhulme Trust (UK) Research Leave Fellowship RF-2013-348 to RES, National Institutes of Health GM113172 grant to M.V.N. and Y.V.B. and R35GM122556 and GM51986 to Y.V.B. AD was supported by an EMBO long term fellowship, WV by funds from the Wellcome Trust (101824/Z/13/Z).

Author Contributions

EK and RES conceived the study and carried out the experiments along with CL using reagents constructed by MvN and JR, and bacterial strains constructed by RT and ADe in WV's lab, who also provided helpful comments. ADu wrote scripts and aided CL and EK with image analysis. YB provided helpful comments and microscopy facilities. RES, EK and CL wrote the manuscript with inputs and comments from the other authors.

Competing Financial interests

The authors declare that there are no competing financial interests.

Figures

Figure 1 a- Biosynthesis of PG starts in the cytoplasm by sequential addition of L-Ala, D-Glu, a diamino acid (e.g. meso-diaminopimelic acid in most Gram-negative bacteria) and a dipeptide of D-Ala-D-Ala to disaccharide units. Once completed, this subunit is then transported to the periplasm to be incorporated into the murein sacculus by glycan polymerisation via transglycosylases. Cross-linking of the glycan strands generally occurs between the carboxyl group of D-Ala at position 4 and the amino group of the diamino acid at position 3, by the action of D,D-transpeptidases. The D-Ala at position 5 can also be cleaved by the actions of D,D-carboxypeptidases. **b-** L,D-transpeptidases cleave the D-Ala from position 4 and utilise the energy from cleaving this bond to form a 3-3 crosslink with another acyl-acceptor stem peptide (for example, a pentapeptide), or replace the D-Ala with a free D-amino acid such as fluorescent D-amino acids (FDAAs). **c** - Timed stages of the predatory cycle of *B. bacteriovorus* (black) bacteria invading *E. coli* prey (gray). 0-15 minutes post-mixing of *B. bacteriovorus* and prey; *B. bacteriovorus* attach and begin to enter the outer layers of the prey. 30 minutes; most of the *B. bacteriovorus* have entered the prey periplasm, modifying the prey cell to form a rounded "bdelloplast". 1-3 hours; *B. bacteriovorus* growth occurs at the expense of the prey cell contents in the form of elongation as a filament. 4 hours; this filament fragments into smaller attack phase cells which break out from the bdelloplast **d-** FDAAs used in this study, colours are representative of emission maxima. **e-** Multi-coloured FFAA labelling

scheme (using excess *B. bacteriovorus* to promote synchronous invasion of prey) with time points observed by wide field epifluorescence microscopy. Predator and prey cells were pre-labelled separately with BADA and TADA respectively before being washed and then mixed. Samples of the mixed infection were then pulse-labelled with HADA for 10 minutes before each time point before being fixed, washed, then microscopically observed. **f-** Phase contrast and epi-fluorescent microscopy images of the early stages of *B. bacteriovorus* predation (20 minutes plus 10 minutes of HADA labelling = 30 minutes post mixing of predators with prey). The *B. bacteriovorus* are false-coloured in green, the *E. coli* prey cells are false-coloured in red and pulsed HADA signal is false-coloured in blue. Each channel is displayed independently in white and with all 3 fluorescence channels merged in epifluorescence (EPI) overlay. HADA fluorescence signal on the prey wall has an intense focus at each point of *B. bacteriovorus* contact and spreads from this point across the rest of the wall. This can also be seen at 15 minutes in Figure 5. The two images are representative of between 321 and 10,546 cells for each timepoint, detailed in **Supplementary Material**.

Figure 2- 3D-SIM images of early predation by *B. bacteriovorus* (pre-labelled with BADA, false-coloured red) on prey *E. coli* cells after a pulse labelling for 10 minutes with HADA (false-coloured cyan) to show early modification of cell walls. **a-** Predation 15 minutes post mixing reveals a ring of HADA-labelled prey cell wall modification at the point of *B. bacteriovorus* contact (arrowheads) and of similar width to the *B. bacteriovorus* cell (see **Supplementary Table 1**) . Central pores in the labelled PG material can be seen where the *B. bacteriovorus* image is artificially removed from the overlay of the two channels. Such annuli may represent a thickened ring of PG modification. In the white inset; the lookup table for the BADA channel has been separately adjusted until all the BADA labelled predators were clearly visible. **b-** Prey PG is deformed around the site of *B. bacteriovorus* invasion (arrowheads). **c-** The cells show HADA fluorescence at the end of the internal *B. bacteriovorus* cell (arrowheads) which likely represents transpeptidase activity re-sealing the hole in the prey PG after the *B. bacteriovorus* cell has entered. Images are representative of >100 3D-reconstructed cells in

two independent experiments (**Supplementary Materials** and **Supplementary Table 1** for details of numbers analysed). Scale bars are 1µm.

Figure 3- 3D-SIM images of early predation by *B. bacteriovorus* (pre-labelled with BADA, false-coloured green) on prey *E. coli imp4213* cells (which are more permeable and thus susceptible to the TADA pre-labelling, false coloured in red) after a pulse labelling for 10 minutes with HADA (false-coloured cyan) to show early modification of cell walls. **a-** FDAA labelling scheme (using excess *B. bacteriovorus* to promote synchronous invasion of *E. coli* $\Delta imp4213$ mutant prey) with time points observed by 3D-SIM fluorescence microscopy. Predator and prey cells were pre-labelled separately with BADA and TADA respectively before being washed and then mixed. Samples of the mixed infection were then pulse-labelled with HADA for 10 minutes before time points up to 30 minutes, the cells were fixed, washed and then microscopically observed. **b-** Predation 30 minutes post mixing with this prey strain reveals a pore in the TADA signal coincident with the ring of HADA-labelled prey cell wall modification at the point of *B. bacteriovorus* contact (arrowheads) and of similar width to the *B. bacteriovorus* cell (**Supplementary Table 2**) . **b-** In several cases (**Supplementary Table 2**) where the *B. bacteriovorus* cell had entered into the prey cell and established itself in the periplasm of the bdelloplast, the pore in the TADA was coincident with a patch of HADA- and thus is likely to represent the sealing of the pore through which the *B. bacteriovorus* had entered.

Figure 4 a- Plot of mean HADA fluorescent signal of cells against time throughout the predation cycle. Measurements are total mean background-corrected fluorescent signal from free swimming wild type *B. bacteriovorus* cells (grey line) or free swimming $\Delta 2ldt$ mutant (yellow line), or total mean background-corrected fluorescent signal of invaded prey bdelloplast (including the signal from the invading *B. bacteriovorus*). Mean fluorescent signal was significantly lower in the bdelloplasts invaded by the $\Delta 2ldt$ mutant (orange line) compared to those invaded by the wild type (blue line) at the 15-45 minute timepoints. Time is in minutes post-mixing of predator and prey and fluorescence is in relative fluorescent

units measured by MicrobeJ. Prey and *B. bacteriovorus* cells were distinguished by filtering based on size (see methods). Data were from at least two independent repeats (see **Supplementary Materials** for details of n). Error bars are standard error of the mean. The HADA signal differences between *E. coli* preyed upon by wt or $\Delta 2ldt$ mutant were significant in each of the time points ($p < 0.0001$ for all time points except 240 min time point, for which $p = 0.016$)

b- Reverse Transcriptase PCR showing the expression of predicted L,D-transpeptidase genes *bd0886* and *bd1176* or control gene *dnaK*, over the predatory cycle of *B. bacteriovorus*. RNA was isolated at the time points indicated across the top of the gel during one round of synchronous *B. bacteriovorus* infection of *E. coli* cells. Primers were designed to anneal specifically to the gene of interest. L = 100bp DNA ladder, AP = Attack Phase cells, 15-45, 1h-4h = minutes or hours respectively since mixing of *B. bacteriovorus* and prey. Ec = *E. coli* strain S17-1 RNA (negative control: no *B. bacteriovorus*); NT = control with no template RNA; Gen = *B. bacteriovorus* HD100 genomic DNA (positive control). The cartoon above represents the different stages of predation. Expression of both genes peaked at 15-30 minutes post-mixing predator and prey. Two independent repeats were carried out and showed the same transcription pattern.

c- FDAA labelling focusing on the stages of *B. bacteriovorus* wild-type HD100 and **d-** $\Delta 2ldt$ mutant predation and bdelloplast establishment. White arrowheads point to HADA modification of the bdelloplast (in the wild-type) and HADA polar foci visible on the mutant predators inside the bdelloplast. The *B. bacteriovorus* are false-coloured in green, the *E. coli* prey cells are false-coloured in red and the HADA pulse-labelling is false-coloured in blue. Each channel is displayed independently and with all 3 fluorescence channels merged. HADA fluorescence of the prey cell during predation with the L,D-transpeptidase mutant is less than for predation by the wild-type. Scale bars are 1 μ m. Images are representative of 5 independent replicates for the wild-type and 2 independent replicates for the Ldt mutant (**Supplementary Material** for details of n).

Figure 5a- Chart of mean HADA fluorescent signal of prey strains preyed upon by *B. bacteriovorus* (+Bd), and pulsed with HADA at 35-45 minutes post mixing (the timepoint of maximal HADA incorporation for *E. coli* S17-1). Controls were in Ca/HEPES buffer without *B. bacteriovorus* predation, but pulsed with HADA at the same timepoint. Measurements are total mean background corrected fluorescent signal of prey cells and is reported in relative fluorescent units measured by MicrobeJ. Prey cells lacking all 6 L,D-transpeptidases ($\Delta 6LDT$) accumulated more HADA fluorescence upon predation by *B. bacteriovorus*. Control samples without *B. bacteriovorus* predation accumulated considerably less HADA fluorescence. Controls of $\Delta 6LDT$ prey cells without *Bdellovibrio* predation accumulated negligible HADA fluorescence. Data were from two (for the controls) or three independent repeats. Error bars are standard error of the means. WT- *E. coli* BW25113 wild-type strain YB7421, 6LDT- *E. coli* BW25113 $\Delta 6LDT$ strain deficient in all 6 L,D transpeptidases, *dacA*- *E. coli* BW25113 strain YB7423 deficient in *DacA*, 6LDT*dacA*- *E. coli* BW25113 $\Delta 6LDT\Delta dacA$ strain YB7439 deficient in all 6 L,D transpeptidases and *dacA*. N/S- not significant; all other comparisons were significant $p < 0.0001$ with the one exception shown.

b- CPRG β -galactosidase assay measuring cytoplasmic leakage of shocked *E. coli* bdelloplasts formed by wild type (BP HD100 WT) or bdelloplasts formed by $\Delta 2ldt$ mutant *B. bacteriovorus* (BP Ldt- mutant) with controls of uninvaded *E. coli* prey cells (S17-1 only) or *B. bacteriovorus* cells alone (HD100 WT only). Red colour from positive CPRG reaction was measured by spectrophotometry at 574 nm and readings were normalised to each experiment. Bdelloplasts were harvested by centrifugation and shocked by resuspension in Ca/HEPES buffer for no shock- except centrifugation only (Buffer), Ca/HEPES buffer supplemented with 750mM NaCl (Upshock) or upshock followed by further centrifugation and resuspension in water (Downshock). Error bars are standard error of the mean. Statistical significance was determined by Student's *t*-test * $p < 0.05$ ** $p < 0.01$ *** $p < 0.001$. Data were the mean of 7 independent repeats.

Figure 6- Phase contrast (**a**) and epi-fluorescent microscopy and 3D-SIM (**b-d**) images of the later stages of *B. bacteriovorus* predation (after the peak of bdelloplast HADA labelling, by wild type predator, has ended). The *B. bacteriovorus* were pre-labelled with BADA and are false-coloured in green, the *E. coli* prey cells were pre-labelled with TADA and are false-coloured in red. The cells were pulse-labelled for 10 minutes before each acquisition timepoint with HADA, which is false-coloured in cyan. Each channel is displayed independently and with all 3 fluorescence channels merged. The HADA fluorescence indicates synthesis of the *B. bacteriovorus* PG, which initiates at many points along the growing predator (2 hours, **b**; red arrowheads) except the poles (2 hours; **b**; green arrowheads), before developing into foci (3 hours; **c**; red arrowheads), which become septa (4 hours; **d**, red arrowhead). After division, newly released *B. bacteriovorus* can be seen to modify their whole PG (4 hours; **d**, white arrowheads). *B. bacteriovorus* that did not invade (there was an excess of *B. bacteriovorus* to ensure efficient predation) can be seen to have a strong BADA signal and low HADA signal (4 hours; **d**, yellow arrowheads). Images are representative examples from thousands of cells from five independent experiments (**a**) and of >100 3D-reconstructed cells in two independent experiments (**b-d**) see **Supplementary Material** for numbers of cells analysed. Scale bars are 1 μ m.

Materials and Methods

RNA isolation from predatory cycle and RT-PCR analysis

Synchronous predatory infections of *B. bacteriovorus* HD100 on *E. coli* S17-1 in Ca/HEPES buffer (2 mM CaCl₂ 25 mM HEPES pH7.6), or strain S17-1 suspended in Ca/HEPES alone, were set up as previously described³⁹ with samples throughout the timecourse being taken and total RNA isolated from them. This semi-quantitative PCR allows the evaluation of specific predator transcripts in the presence of fluctuating levels of prey RNA as the predator degrades it. RNA was isolated from the samples using a Promega SV total RNA isolation kit with the RNA quality being verified by an Agilent Bioanalyser using the RNA Nano kit. RT-PCR was performed with the Qiagen One-step RT-PCR kit with the following reaction conditions: One

cycle 50°C for 30 minutes, 95°C for 15 minutes, then 25 cycles of 94°C for 1 min, 50°C for 1 min, 72°C for 1 min, and finally a 10 minutes extension at 72°C after the 30 cycles, and finally a 4°C hold. All experiments were carried out with at least 2 independent repeats. Primers to anneal to *bd0886* were 5'- AGCCTCTACATGGGTGCAAG -3' and 5'- AACTTGGCTGCATACCAACC -3'. Primers to anneal to *bd1176* were 5'- GCCAACGCCAGCGTGAATGC-3' and 5'-GGCCGTCGTTGAGTTGCTGC-3'.

534 **Generating gene deletion mutants in *B. bacteriovorus***

Markerless deletion of both the *bd0886* and *bd1176* genes from *B. bacteriovorus* HD100 was achieved sequentially as described previously^{22,40}. Primers designed to amplify to the upstream region of *bd0886* were: Bd0886F 5'-ACGGGGTACCCACGATCCCATCTTATAAGC -3' and

Delbd0886F 5'-GGAGATTATATGAAAGCTTTCTAGAATGGACTCTGTTCTGCGC-3'.

Primers designed to amplify to the downstream region of *bd0886* were:

Delbd0886R 5'-GCGCAGGAACAGAGTCCATTCTAGAAAGCTTTCATATAATCTCC-3' and

Bd0886R 5'-CTGTAGCATGC TTCAGATCCTCGCTGAAACC-3'

Primers designed to amplify to the upstream region of *bd1176* were: Bd1176-F 5'- GCGCAAAAGCTTTCGCAAGCTGGGTGTTTCAGC -3' and

Delbd1176F 5'- GATTGCCAGCTCCCCTATGTCTAGAAATCCTCCGAAGATCGTTT -3'.

Primers designed to amplify to the downstream region of *bd1176* were:

Delbd1176R 5'- AAACGATCTTCGGAGGATTTCTAGACATAGGGGAGCTGGCAATC -3' and

Bd1176-R 5'- ACGGGGTACCGGATGTGATTCATACCAGCC-3'

549 **Construction of an *E. coli* strain lacking all 6 LD-transpeptidases**

E. coli BW25113Δ6LDT lacks all five previously published LD-transpeptidase genes (*erfK*, *ybiS*, *ycfS*, *ynhG*, *ycbB*)^{15,41} plus a sixth gene encoding a putative LD-transpeptidase, *yafK*. Gene deletions were generated and combined by transferring *kan*-marked alleles from the Keio *E. coli* single-gene knockout library⁴² into relevant background strains using P1 phage

transduction⁴³. The Keio pKD13-derived *kan* cassette is flanked by FRT sites, allowing removal of the *kan* marker via expression of FLP recombinase from plasmid pCP20 to generate unmarked deletions with a FRT-site scar sequence^{42,44}. The gene deletions present in BW25113Δ6LDT were verified by PCR, and the analysis of the PG composition showed that muropeptides generated by the activities LD-transpeptidases were below the limit of detection.

Fluorescent tagging of Bd1176

The *bd1176* gene was cloned into the conjugable vector pK18*mobsacB* such a way as to fuse the genes at the C-terminus with the mCherry gene. This fusion was introduced into *B. bacteriovorus* by conjugation as described previously⁴⁵. Cloning was carried out using the NEB Gibson cloning assembly kit and the primers used (5'-3') were: cgttgtaaaacgacggccagtgccATGACAAAGATTAATACGCGCC, ccttgctcaccatGTTGTTGCCGCTCTTCTTG, aggcggcaacaacATGGTGAGCAAGGGCGAG and cagctatgacatgattacgTTACTTGTACAGCTCGTCCATGCC Epi-fluorescence microscopy was undertaken using a Nikon Eclipse E600 through a 100x objective (NA 1.25) and acquired using a Hamamatsu Orca ER Camera. Images were captured using Simple PCI software (version 6.6). An hcRED filter block (excitation: 550-600 nm; emission: 610-665 nm) was used for visualisation of mCherry tags.

Labelling of cells with FDAAs and imaging

Bdellovibrio bacteriovorus HD100 cells were grown predatorily for 16 hours at 30°C on stationary phase *E. coli* S17-1 prey, until these were lysed. The *B. bacteriovorus* were then filtered through a 0.45 µm filter (yielding ~2 x 10⁸ pfu per ml) and concentrated 30 x by centrifugation at 12,000 x *g* for 5 minutes. The resulting pellet was resuspended in Ca/HEPES buffer, (2 mM CaCl₂ 25 mM HEPES pH7.6) and then pre-labelled with a final concentration of 500 µM BADA (by addition of 5 µl of a 50 mM stock in DMSO) for 30 minutes at 30°C. The cells were then washed twice in Ca/HEPES buffer before being resuspended in an equal

580 volume of Ca/HEPES buffer. *E. coli* S17-1 or *E. coli imp4213* cells were grown for 16 hours in
 581 LB at 37°C with shaking at 100 rpm were back diluted to OD₆₀₀ 1.0 in fresh LB, (yielding ~1 x
 582 10⁹ cfu per ml) and labelled with final concentration of 500 µM TADA (by addition of 5 µl of a
 583 50 mM stock in DMSO) for 30 minutes at 30°C, before being washed twice in Ca/HEPES
 584 buffer then resuspended in an equal volume of Ca/HEPES buffer. *E. coli* BW25113 strains
 585 were grown as for strain S17-1, except strains YB7423, YB7424 and YB7439 were
 586 supplemented with 50 µg per ml kanamycin sulphate for incubation and washed of this by
 587 centrifugation at 5,000 x g for 5 minutes, resuspension in an equal volume of LB broth and
 588 further centrifugation at 12,000 x g for 5 minutes before back-dilution to OD₆₀₀ 1.0 in
 589 Ca/HEPES buffer. This resulted in similar numbers of cells for each strain; *E. coli* BW25113
 590 Δ6LDT 5.1 x 10⁸ ± 3.6 x 10⁷, YB7423 5.2 x 10⁸ ± 1.8 x 10⁸, YB7424 4.9 x 10⁸ ± 2 x 10⁷,
 591 YB7439 4.3 x 10⁸ ± 1.6 x 10⁸ as determined by colony forming units.

592 Defined ratios of approximately 5 *B. bacteriovorus* predators to 1 *E. coli* prey were then
 593 prepared for semi-synchronous predation experiments to allow FDAA labelling of dynamic PG
 594 changes as the predators were invading and replicating within the prey. Five hundred
 595 microlitres of the pre-labelled *B. bacteriovorus* were mixed with 400 µl of the pre-labelled *E.*
 596 *coli* and 300 µl of Ca/HEPES buffer and incubated at 30°C. For HADA pulse-labelling, 120 µl
 597 samples of these predatory cultures were added to 1.2 µl of a 50 mM stock of HADA in DMSO
 598 10 minutes before each sampling timepoint for microscopy and returned to 30°C incubation.
 599 These experimental timescales are consistent and shown in diagram above figures (for
 600 example 30 minute predation timepoint = 20 minutes of predator mixed with prey, plus 10
 601 minutes of subsequent HADA labelling, followed by immediate fixation and washing). At the
 602 timepoint, all the 120 µl predator-prey sample was transferred to 175 µl ice cold ethanol and
 603 incubated at -20°C >15 minutes to fix the cells. The cells were pelleted by centrifugation at
 604 12,000 x g for 5 minutes, washed with 500 µl PBS and resuspended in 5 µl Slowfade
 605 (Molecular Probes Ltd) and stored at -20°C before imaging. 2 µl samples were imaged using
 606 a Nikon Ti-E inverted fluorescence microscope equipped with a Plan Apo 60x/1.40 Oil Ph3

DM objective, 1.5x intermediate magnification, a CFP/YFP filter cube and an Andor DU885 EMCCD camera using CFP settings for detection of HADA (emission maximum 450 nm), a FITC filter cube for detection of BADA (emission maximum 512 nm) and others. Later timepoints were prepared with similar HADA pulses carried out on further samples of the continuing predator- prey culture which extended to 4 hours of incubation at 30°C; the point at which new *B. bacteriovorus* predators emerge from lysed *E. coli* prey.

Super resolution microscopy

3D Structured illumination microscopy was performed using a DeltaVision OMX Imaging System equipped with an Olympus UPlanSApo 100X/1.40 Oil PSF objective and a Photometrics Cascade II EMCCD camera. The samples were excited with lasers at 405 nm, 488 nm, 561 nm and the emission was detected through 419 nm-465 nm, 500 nm-550 nm, 609 nm-654 nm emission filters. The image processing was conducted by SoftWorx imaging software. Further image analysis and processing was conducted via ImageJ or Icy (<http://www.bioimageanalysis.org/>).

Quantitation of fluorescent signal

For quantitation of fluorescent signal, images were acquired as above, but with unvarying exposure and gain settings. The exposures were chosen to give values that did not exceed the maximum so that saturation was not reached for any of the fluorescent channels. Images were analysed using the MicrobeJ plugin for the ImageJ (FIJI distribution) software (<http://www.indiana.edu/~microbej/index.html>)⁴⁶ which automates detection of bacteria within an image. The *E. coli* prey cells and *Bdellovibrio* cells were detected using the resulting binary mask from both the phase contrast and either the TADA or the BADA channels respectively. The *E. coli* prey cells and *B. bacteriovorus* cells were differentiated by defining two cell types based on size; Cell Type 1 (for *E. coli*) were defined by area 0.9-6 μm^2 , length 1.5-7 μm , width 0.4-3 μm and all other parameters as default; Cell Type 2 (for the smaller *B. bacteriovorus* cells) were defined by area 0-1 μm^2 , length 0.5-1.5 μm , width 0.2-0.8 μm and all other parameters as default. Manual inspection of the analysed images confirmed that the vast majority of cells were correctly assigned, but that only unattached cells were recognised

and measured. *Bdellovibrio* cells were linked hierarchically with the *E. coli* prey cells, in order to distinguish between internalized, attached and unattached predator cells. The shape measurements including the angularity, area, aspect ratio, circularity, curvature, length, roundness, sinuosity, solidity and width were measured for each type of cell. Background-corrected mean fluorescent intensity was measured for each cell and then the mean of these measurements was determined for each cell type, for each independent experiment. Typically, 500-5,000 cells were measured at each timepoint for each independent experiment (details of n for each sample in each experiment are presented in **Supplementary Materials**).

CPRG assay of leakage of osmotically shocked bdelloplasts derived from predation by Ldt mutant versus wild type *B. bacteriovorus*.

To evaluate whether DAA transfer to prey bdelloplast cell walls altered the physical stability of those walls to osmotic changes, an assay for leakage of cytoplasmic contents, including β -galactosidase was used, with the CPRG as a detection reagent.

E. coli S17-1 (*lac*⁺) prey cells were grown for 16 hours in YT broth at 37°C with 200 rpm shaking, before being supplemented with 200 μgml^{-1} IPTG for 2 hours to induce expression of *lacZ*. These prey cells were then centrifuged at 5,100 x *g* for 5 minutes and resuspended in Ca/HEPES buffer (2 mM CaCl₂ 25 mM HEPES pH7.6) then diluted to OD₆₀₀ 1.0 in Ca/HEPES buffer. *Bdellovibrio bacteriovorus* HD100 or Ldt⁻ strains were grown predatorily for 16 hours at 29°C on stationary phase *E. coli* S17-1 prey until these were fully lysed, and then *B. bacteriovorus* were filtered through a 0.45 μm filter, concentrated 50 x by centrifugation at 5,100 x *g* for 20 minutes and resuspended in Ca/HEPES buffer. Total protein concentration of these concentrated suspensions was determined by Lowry assay, and matched amounts of 50 μg of each strain were used for semi-synchronous infections (between 115 and 284 μl of concentrated suspension made up to a total of 800 μl in Ca/HEPES buffer) with 400 μl of diluted *E. coli* S17-1 prey cells. This resulted in a multiplicity of infection (MOI of *B. bacteriovorus* cells : *E. coli* cells) of 1.4 to 10.5 for the wild-type strain HD100 as determined by plaque assay. The excess of predators resulted in >99.4% of *E.coli* prey cells rounded by

663 invasion of strain HD100 and >99.6% of prey cells rounded by invasion of Ldt mutant after
664 incubation at 29°C for 1 hour with shaking at 200 rpm.

665 A control of prey only (400 µl diluted prey cells with 800 µl Ca/HEPES buffer) resulted in no
666 rounded prey cells and a control of wild-type *B. bacteriovorus* HD100 cells only (50 µg in a
667 total of 1200 µl Ca/HEPES buffer) was included. After incubation, bdelloplasts (or cells in the
668 controls) were harvested by centrifugation at 17,000 x *g* for 2 minutes and supernatant
669 removed. The pellets were resuspended in: 1) Ca/HEPES buffer supplemented with 20 µgml⁻¹
670 ¹ CPRG (Sigma) for centrifugation shock only 2) Ca/HEPES buffer supplemented with 750mM
671 NaCl and 20 µgml⁻¹ CPRG for upshock 3) Ca/HEPES buffer supplemented with 750mM NaCl,
672 incubated for 30 minutes at 29°C followed by centrifugation at 17,000 x *g* for 2 minutes and
673 supernatant removed, then the pellet resuspended in water supplemented with 20 µgml⁻¹
674 CPRG for downshock. These were then incubated for 30 minutes at 29°C before purifying the
675 supernatant, containing any bdelloplast leakage products, for β-galactosidase assay by
676 removing cells by centrifugation at 17,000 x *g* for 2 minutes followed by filtration through a 0.2
677 µm filter. The β-galactosidase assay was carried out by incubation at 29°C for 26 hours and
678 colour change was monitored by spectrophotometry at 574 nm. Data were normalised for each
679 experiment.

680 Extra experimental considerations: The Ldt mutant strain exhibited a plaquing phenotype,
681 forming mostly very small plaques with ~1% forming larger plaques similar to the wild-type
682 HD100 strain (see **Supplementary Figure 6**) and as such an accurate MOI could not be
683 measured by plaques for this strain. To confirm that matching the input cells by Lowry assay
684 resulted in similar numbers of *B. bacteriovorus*, and therefore a similar MOI, images of the
685 mixed prey and predators were analysed. After the 1 hour incubation at 29°C, 40 µl samples
686 were mixed with 2 µl of 0.3 µm polystyrene beads (Sigma; diluted 500 x and washed 5 x with
687 water). 10 µl samples were dropped onto microscope slides with a 1% agarose pad made with
688 Ca/HEPES buffer and 20 fields of view were imaged at 1000 x phase contrast with a Nikon Ti-
689 E inverted microscope. Images were analysed with the MicrobeJ plugin as described above,

but including a third cell type definition for quantifying the beads defined by area 0-1, length 0.1-0.8, width 0.1-0.6 and all other parameters 0-max. This confirmed that there were not significantly different ratios of beads to *B. bacteriovorus* cells in the two strains (6.1 ± 3.9 for HD100, 6.9 ± 0.7 for Ldt mutant) and that all visible prey cells were rounded up after 1 hour of incubation, indicating that an MOI of >1 was achieved (which was required for semi-synchronous infection). To confirm that the defective plaquing phenotype of the Ldt mutant was not a result of low yield in liquid culture, images were analysed at the start and end of predatory growth in liquid. The average result of 5 Lowry assays was taken to match the starting amounts of *B. bacteriovorus*: 245 μ l of strain HD100 and 337 μ l of the Ldt mutant strain (after filtration through a 0.45 μ m filter, but not concentrated) were made up to 800 μ l in Ca/HEPES buffer and added to 400 μ l prey *E. coli* diluted to OD₆₀₀ 1.0 in Ca/HEPES buffer. This mix was imaged with beads as described above at time 0 and 24 hours (after incubation at 29°C with 200 rpm shaking) and analysed using the MicrobeJ plugin as described above. The increase in numbers of *B. bacteriovorus* cells per bead was not significantly different between the 2 strains (1.9 ± 0.5 for HD100 and 2.1 ± 0.8 for the Ldt mutant). In both cases, the prey cells were almost eradicated after 24 hours with only 8-13 cells detected by microbeJ in the 20 fields of view for each experiment (reduced to 1.0 ± 0.4 % of starting values for HD100 and 3.3 ± 0.8 % for the Ldt mutant).)

References

- 1 Vollmer, W., Blanot, D. & de Pedro, M. A. Peptidoglycan structure and architecture. *FEMS Microbiol Rev* **32**, 149-167, doi:10.1111/j.1574-6976.2007.00094.x (2008).
- 2 Mainardi, J. L. *et al.* A novel peptidoglycan cross-linking enzyme for a beta-lactam-resistant transpeptidation pathway. *J Biol Chem* **280**, 38146-38152, doi:10.1074/jbc.M507384200 (2005).
- 3 Cava, F., de Pedro, M. A., Lam, H., Davis, B. M. & Waldor, M. K. Distinct pathways for modification of the bacterial cell wall by non-canonical D-amino acids. *The EMBO Journal* **30**, 3442-3453, doi:10.1038/emboj.2011.246 (2011).
- 4 Magnet, S. *et al.* Specificity of L,D-transpeptidases from gram-positive bacteria producing different peptidoglycan chemotypes. *J Biol Chem* **282**, 13151-13159, doi:10.1074/jbc.M610911200 (2007).
- 5 Fura, J. M., Kearns, D. & Pires, M. M. D-amino acid probes for penicillin binding protein-based bacterial surface labeling. *J Biol Chem* **290**, 30540-30550, doi:10.1074/jbc.M115.683342 (2015).

723 6 Gupta, R. *et al.* sanThe *Mycobacterium tuberculosis* protein LdtMt2 is a nonclassical
724 transpeptidase required for virulence and resistance to amoxicillin. *Nature medicine* **16**, 466-
725 469, doi:10.1038/nm.2120 (2010).

726 7 Peltier, J. *et al.* *Clostridium difficile* has an original peptidoglycan structure with a high level
727 of N-acetylglucosamine deacetylation and mainly 3-3 cross-links. *J Biol Chem* **286**, 29053-
728 29062, doi:10.1074/jbc.M111.259150 (2011).

729 8 Lam, H. *et al.* D-amino acids govern stationary phase cell wall remodeling in bacteria. *Science*
730 **325**, 1552-1555, doi:10.1126/science.1178123 (2009).

731 9 Radkov, A. D. & Moe, L. A. Bacterial synthesis of D-amino acids. *Appl Microbiol Biotechnol*
732 **98**, 5363-5374, doi:10.1007/s00253-014-5726-3 (2014).

733 10 Kuru, E., Tekkam, S., Hall, E., Brun, Y. V. & Van Nieuwenhze, M. S. Synthesis of fluorescent D-
734 amino acids and their use for probing peptidoglycan synthesis and bacterial growth in situ.
735 *Nature protocols* **10**, 33-52, doi:10.1038/nprot.2014.197 (2015).

736 11 Fleurie, A. *et al.* MapZ marks the division sites and positions FtsZ rings in *Streptococcus*
737 *pneumoniae*. *Nature* **516**, 259-262, doi:10.1038/nature13966 (2014).

738 12 Tsui, H. C. *et al.* Pbp2x localizes separately from Pbp2b and other peptidoglycan synthesis
739 proteins during later stages of cell division of D39. *Mol Microbiol* **94**, 21-40,
740 doi:10.1111/mmi.12745 (2014).

741 13 Pilhofer, M. *et al.* Discovery of chlamydial peptidoglycan reveals bacteria with murein sacculi
742 but without FtsZ. *Nature communications* **4**, 2856, doi:10.1038/ncomms3856 (2013).

743 14 Sanders, A. N. & Pavelka, M. S. Phenotypic analysis of *Escherichia coli* mutants lacking L,D-
744 transpeptidases. *Microbiology* **159**, 1842-1852, doi:10.1099/mic.0.069211-0 (2013).

745 15 Magnet, S. *et al.* Identification of the L,D-transpeptidases responsible for attachment of the
746 Braun lipoprotein to *Escherichia coli* peptidoglycan. *J Bacteriol* **189**, 3927-3931,
747 doi:10.1128/JB.00084-07 (2007).

748 16 Willis, A. R. *et al.* Injections of Predatory Bacteria Work Alongside Host Immune Cells to
749 Treat Shigella Infection in Zebrafish Larvae. *Curr Biol* **26**, 3343-3351,
750 doi:10.1016/j.cub.2016.09.067 (2016).

751 17 Stolp, H. & Starr, M. P. *Bdellovibrio bacteriovorus* gen. et sp. n., a predatory, ectoparasitic,
752 and bacteriolytic microorganism. *Antonie van Leeuwenhoek Journal of Microbiology and*
753 *Seriology* **29**, 217-248 (1963).

754 18 Sockett, R. E. Predatory lifestyle of *Bdellovibrio bacteriovorus*. *Annu Rev Microbiol* **63**, 523-
755 539, doi:10.1146/annurev.micro.091208.073346 (2009).

756 19 Rittenberg, S. C. & Shilo, M. Early host damage in the infection cycle of *Bdellovibrio*
757 *bacteriovorus*. *J Bacteriol* **102**, 149-160 (1970).

758 20 Abram, D., Castro e Melo, J. & Chou, D. Penetration of *Bdellovibrio bacteriovorus* into host
759 cells. *J Bacteriol* **118**, 663-680 (1974).

760 21 Abram, D. & Davis, B. K. Structural properties and features of parasitic *Bdellovibrio*
761 *bacteriovorus*. *J Bacteriol* **104**, 948-965 (1970).

762 22 Lerner, T. R. *et al.* Specialized peptidoglycan hydrolases sculpt the intra-bacterial niche of
763 predatory *Bdellovibrio* and increase population fitness. *PLoS pathogens* **8**, e1002524,
764 doi:10.1371/journal.ppat.1002524 (2012).

765 23 Lambert, C. *et al.* Ankyrin-mediated self-protection during cell invasion by the bacterial
766 predator *Bdellovibrio bacteriovorus*. *Nature communications* **6**, 8884,
767 doi:10.1038/ncomms9884 (2015).

768 24 Lambert, C. *et al.* Interrupting peptidoglycan deacetylation during *Bdellovibrio* predator-prey
769 interaction prevents ultimate destruction of prey wall, liberating bacterial-ghosts. *Sci Rep* **6**,
770 26010, doi:10.1038/srep26010 (2016).

771 25 Evans, K. J., Lambert, C. & Sockett, R. E. Predation by *Bdellovibrio bacteriovorus* HD100
772 requires type IV pili. *J Bacteriol* **189**, 4850-4859, doi:10.1128/JB.01942-06 [pii]10.1128/JB.01942-06
773 (2007).

774 26 Koval, S. F. *et al.* *Bdellovibrio exovorus* sp. nov., a novel predator of *Caulobacter crescentus*.
775 *Int J Syst Evol Microbiol* **63**, 146-151, doi:10.1099/ij.s.0.039701-0 (2013).

776 27 Thomashow, M. F. & Rittenberg, S. C. Intraperiplasmic growth of *Bdellovibrio bacteriovorus*
777 109J: solubilization of *Escherichia coli* peptidoglycan. *J Bacteriol* **135**, 998-1007 (1978).

778 28 Volle, C. B., Ferguson, M. A., Aidala, K. E., Spain, E. M. & Nunez, M. E. Quantitative changes
779 in the elasticity and adhesive properties of *Escherichia coli* ZK1056 prey cells during
780 predation by *Bdellovibrio bacteriovorus* 109J. *Langmuir : the ACS journal of surfaces and*
781 *colloids* **24**, 8102-8110, doi:10.1021/la8009354 (2008).

782 29 Lambert, C., Chang, C. Y., Capeness, M. J. & Sockett, R. E. The first bite-profiling the
783 predatosome in the bacterial pathogen *Bdellovibrio*. *PloS one* **5**, e8599,
784 doi:10.1371/journal.pone.0008599 (2010).

785 30 Sanders, A. N. & Pavelka, M. S. Phenotypic analysis of *Escherichia coli* mutants lacking L,D-
786 transpeptidases. *Microbiology* **159**, 1842-1852, doi:10.1099/mic.0.069211-0 (2013).

787 31 Araki, Y. & Ruby, E. G. A soluble enzyme activity that attaches free diaminopimelic acid to
788 bdelloplast peptidoglycan. *Biochemistry* **27**, 2624-2629 (1988).

789 32 Pilizota, T. & Shaevitz, J. W. Origins of *Escherichia coli* growth rate and cell shape changes at
790 high external osmolality. *Biophys J* **107**, 1962-1969, doi:10.1016/j.bpj.2014.08.025 (2014).

791 33 Pilizota, T. & Shaevitz, J. W. Plasmolysis and cell shape depend on solute outer-membrane
792 permeability during hyperosmotic shock in *E. coli*. *Biophys J* **104**, 2733-2742,
793 doi:10.1016/j.bpj.2013.05.011 (2013).

794 34 Fenton, A. K., Kanna, M., Woods, R. D., Aizawa, S. I. & Sockett, R. E. Shadowing the actions of
795 a predator: backlit fluorescent microscopy reveals synchronous nonbinary septation of
796 predatory *Bdellovibrio* inside prey and exit through discrete bdelloplast pores. *J Bacteriol*
797 **192**, 6329-6335, doi:JB.00914-10 [pii]10.1128/JB.00914-10 (2010).

798 35 Shilo, M. Morphological and physiological aspects of the interaction of bdellovibrio with host
799 bacteria. *Current topics in microbiology and immunology* **50**, 174-204 (1969).

800 36 Iida, Y. *et al.* Roles of multiple flagellins in flagellar formation and flagellar growth post
801 bdelloplast lysis in *Bdellovibrio bacteriovorus*. *J Mol Biol* **394**, 1011-1021, doi:[pii]
802 10.1016/j.jmb.2009.10.003 (2009).

803 37 Eksztejn, M. & Varon, M. Elongation and cell division in *Bdellovibrio bacteriovorus*. *Arch*
804 *Microbiol* **114**, 175-181 (1977).

805 38 Kuru, E. *et al.* In Situ probing of newly synthesized peptidoglycan in live bacteria with
806 fluorescent D-amino acids. *Angewandte Chemie* **51**, 12519-12523,
807 doi:10.1002/anie.201206749 (2012).

808 39 Lambert, C. *et al.* Characterizing the flagellar filament and the role of motility in bacterial
809 prey-penetration by *Bdellovibrio bacteriovorus*. *Molecular Microbiology* **60**, 274-286,
810 doi:MMI5081 [pii]10.1111/j.1365-2958.2006.05081.x (2006).

811 40 Lambert, C. & Sockett, R. Nucleases in *Bdellovibrio bacteriovorus* contribute towards
812 efficient self-biofilm formation and eradication of pre-formed prey biofilms. *FEMS*
813 *Microbiology Letters*, doi:10.1111/1574-6968.12075 (2013).

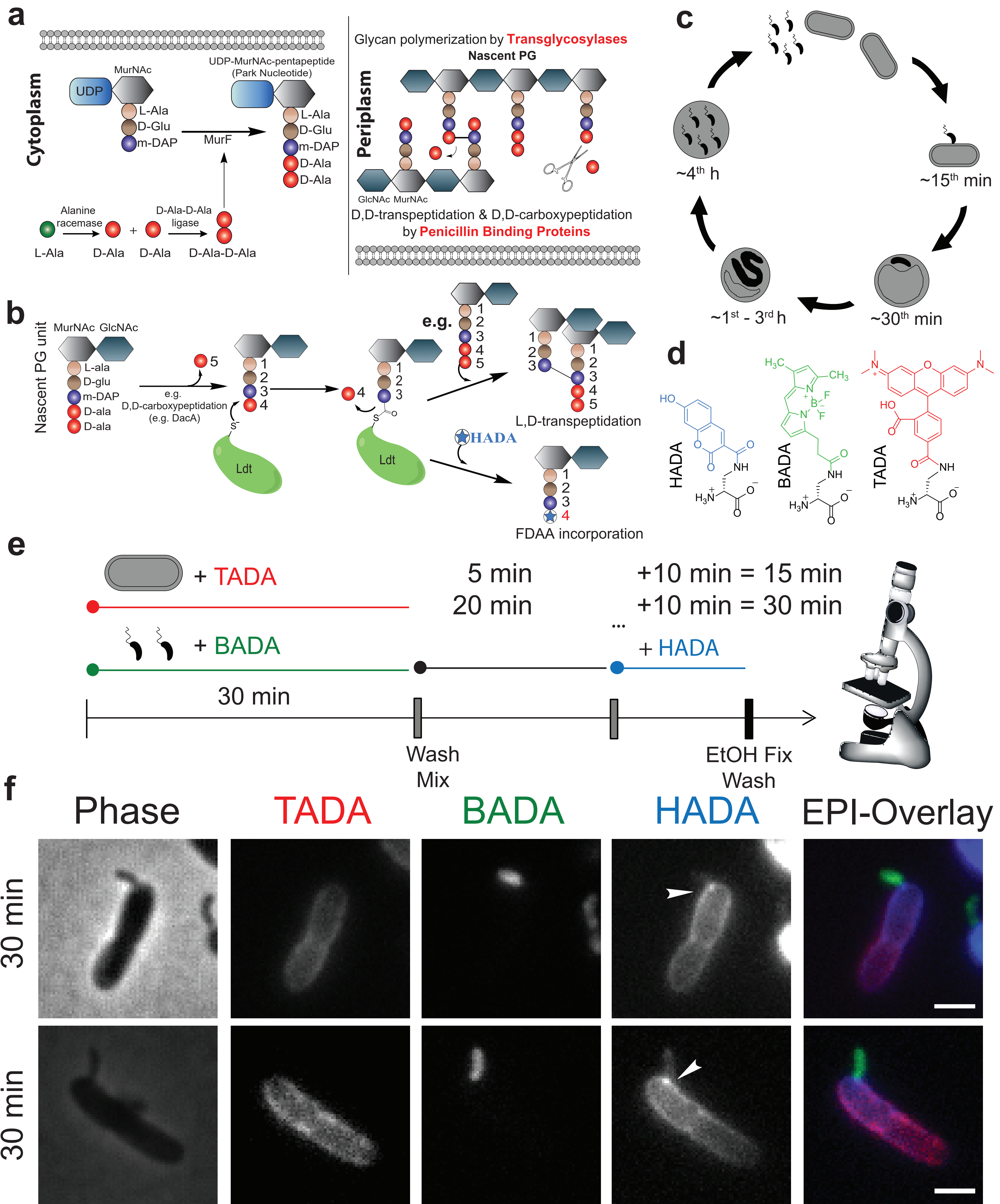
814 41 Magnet, S., Dubost, L., Marie, A., Arthur, M. & Gutmann, L. Identification of the L,D-
815 transpeptidases for peptidoglycan cross-linking in *Escherichia coli*. *J Bacteriol* **190**, 4782-
816 4785, doi:10.1128/JB.00025-08 (2008).

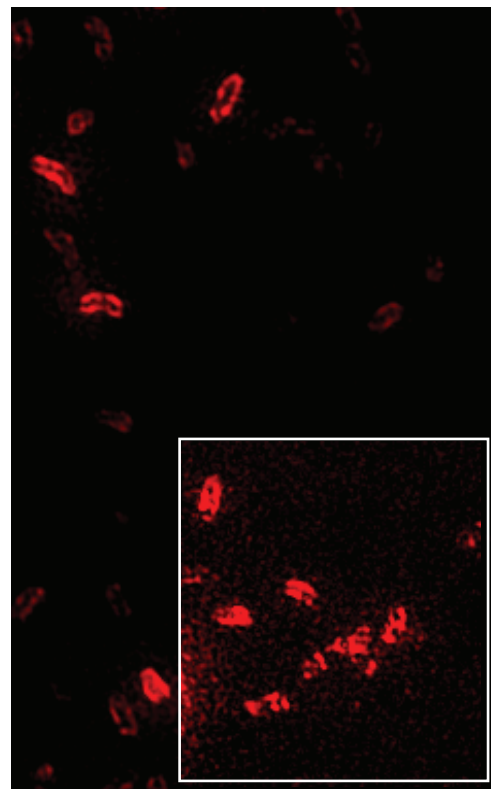
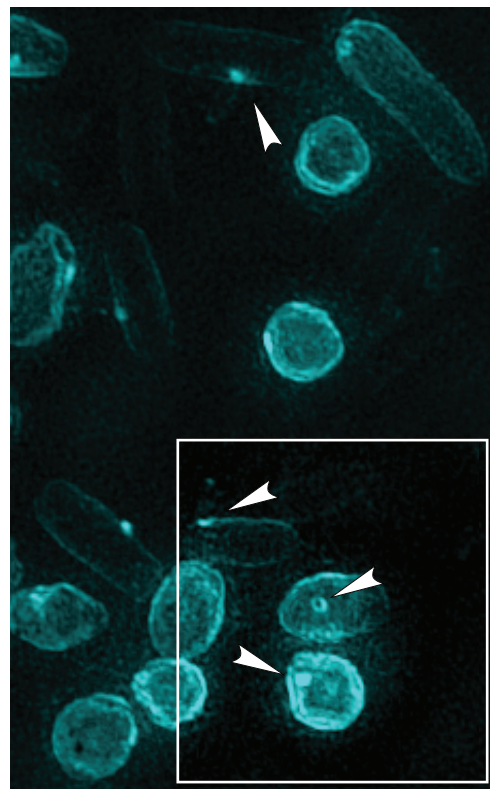
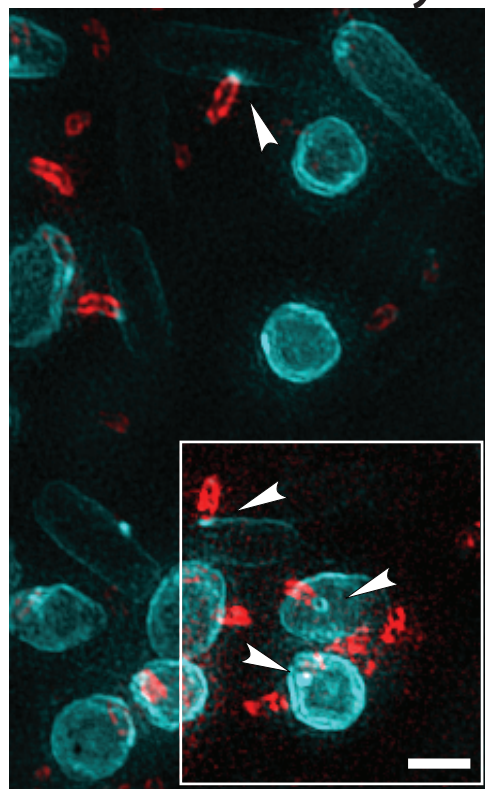
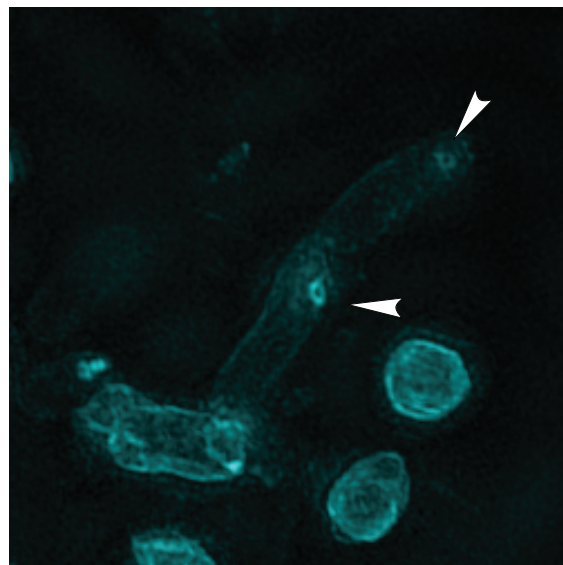
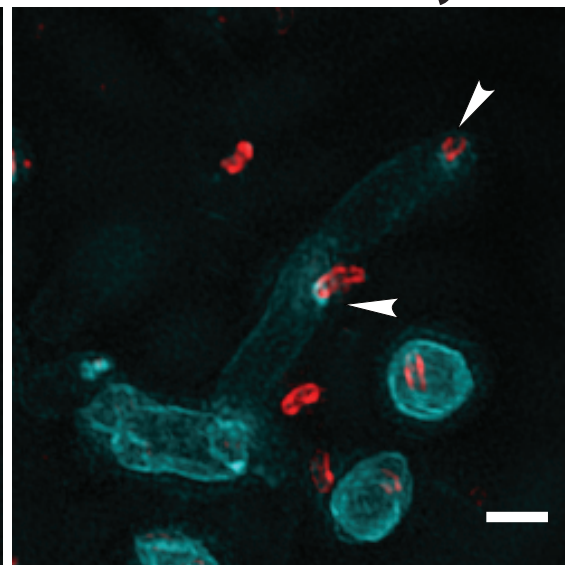
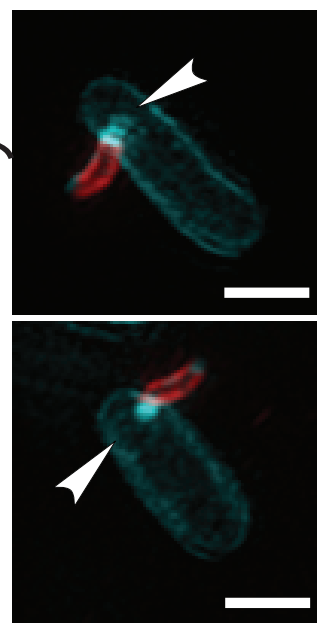
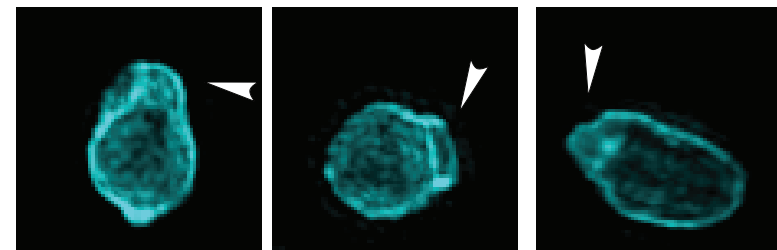
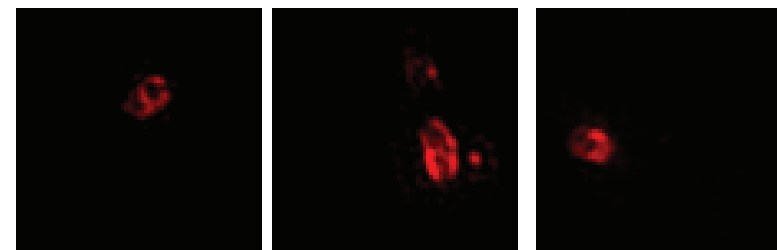
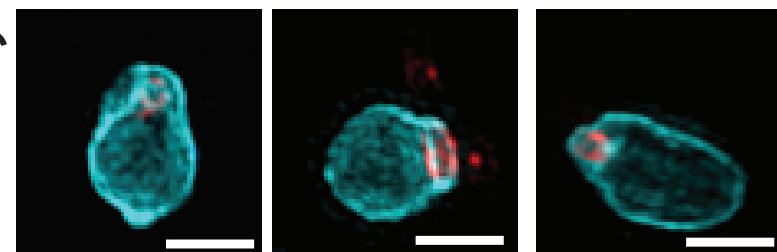
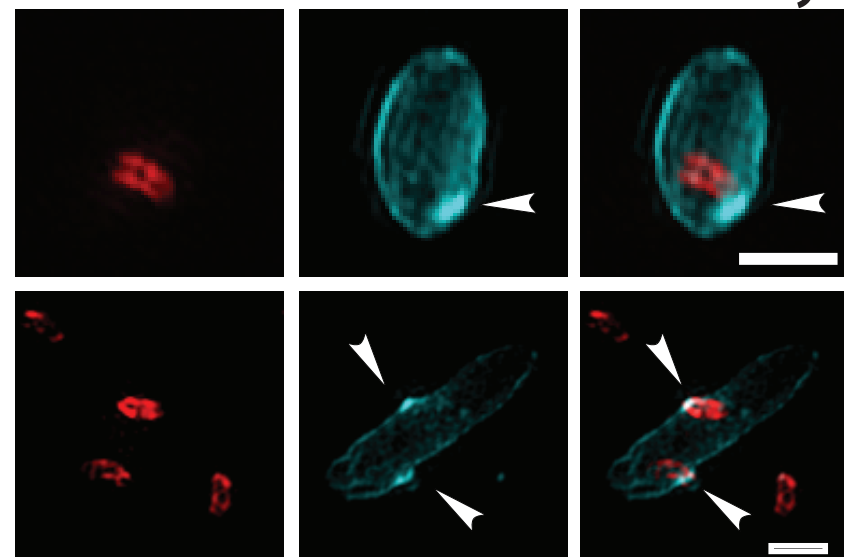
817 42 Baba, T. *et al.* Construction of *Escherichia coli* K-12 in-frame, single-gene knockout mutants:
818 the Keio collection. *Mol Syst Biol* **2**, 2006 0008, doi:10.1038/msb4100050 (2006).

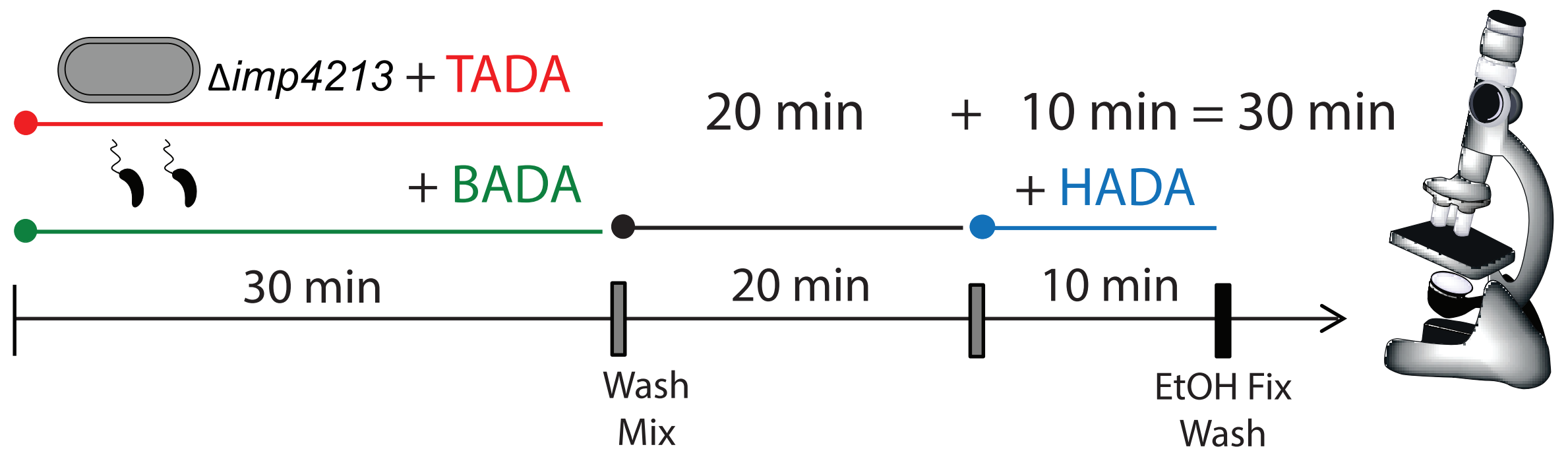
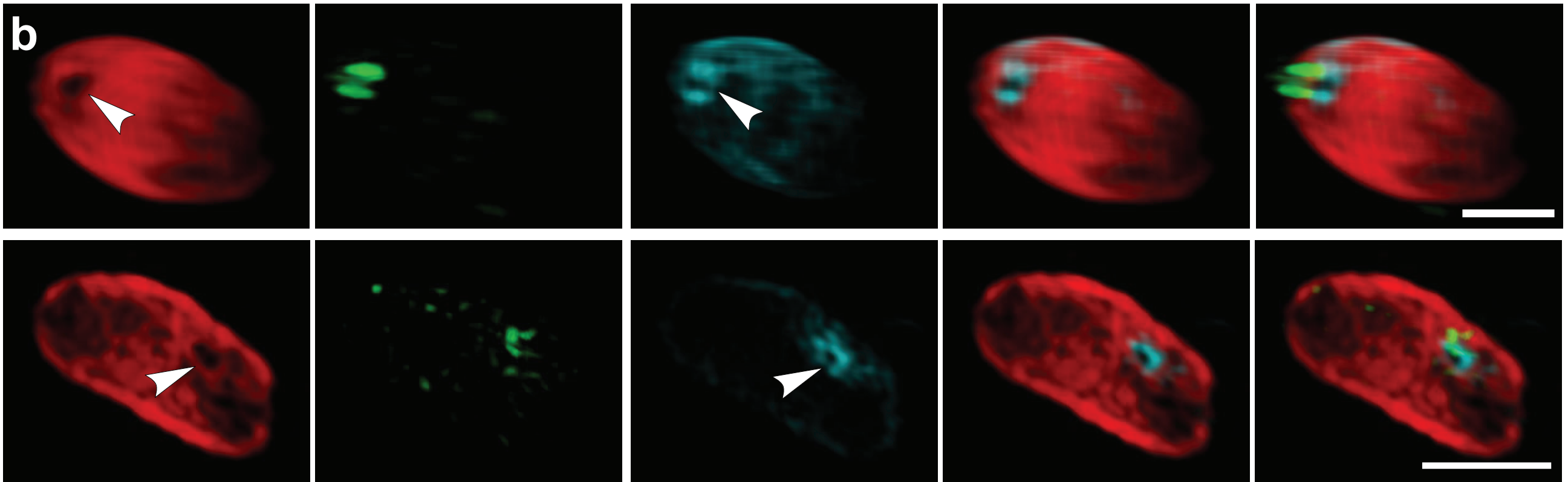
819 43 LC, T., JA, S., X, L., N, C. & DL, C. Recombineering: genetic engineering in bacteria using
820 homologous recombination. *Curr Protoc Mol Biol* **14**, 1-39 (2014).

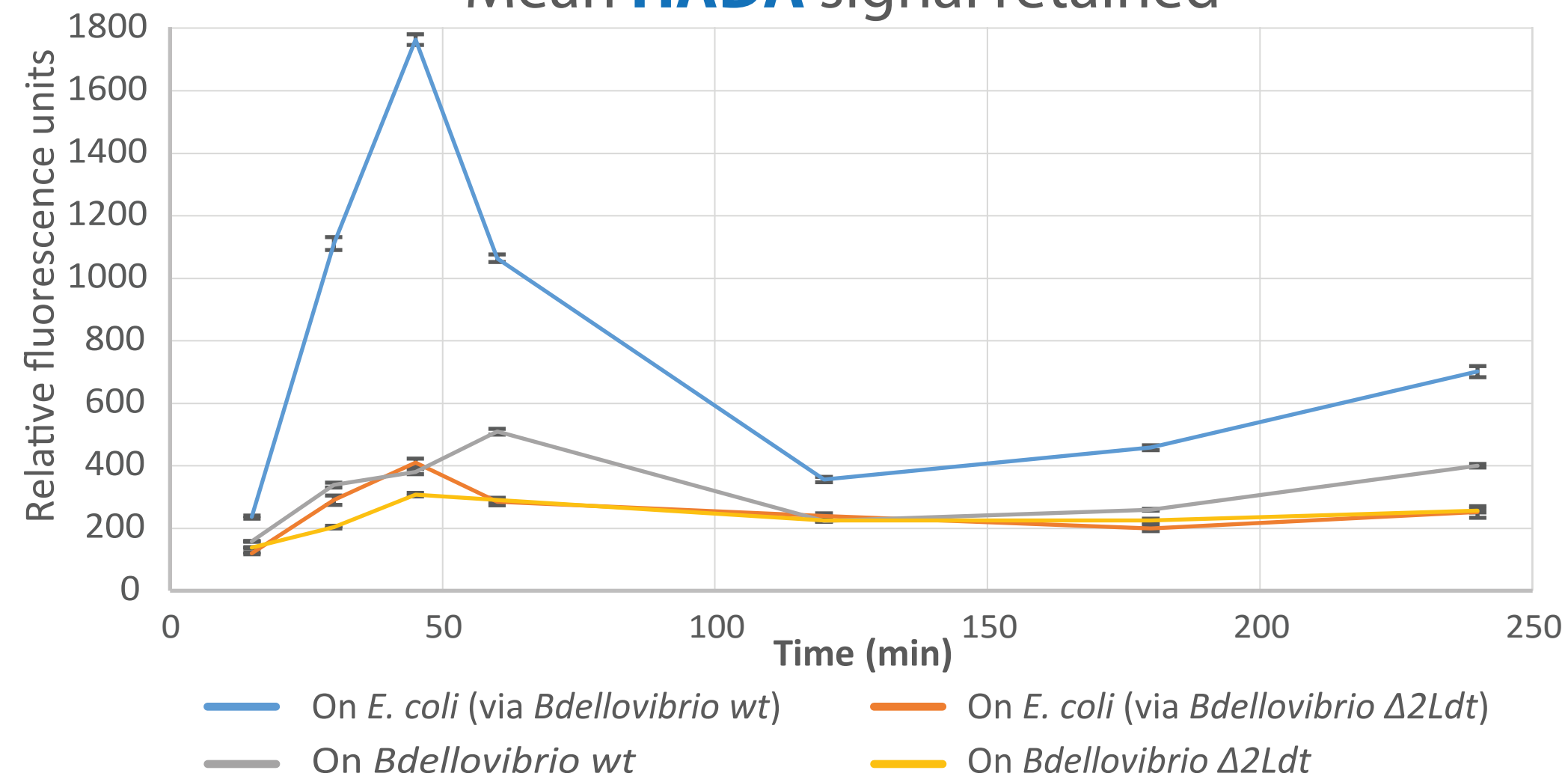
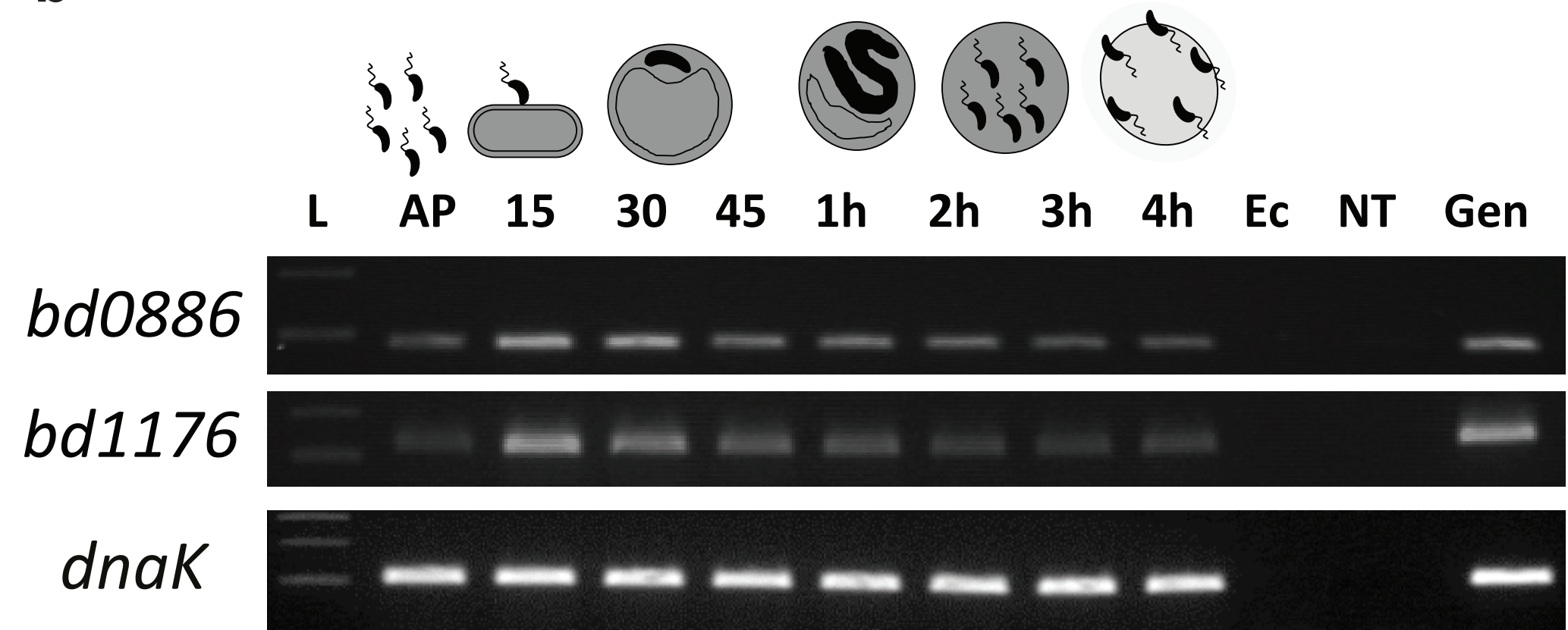
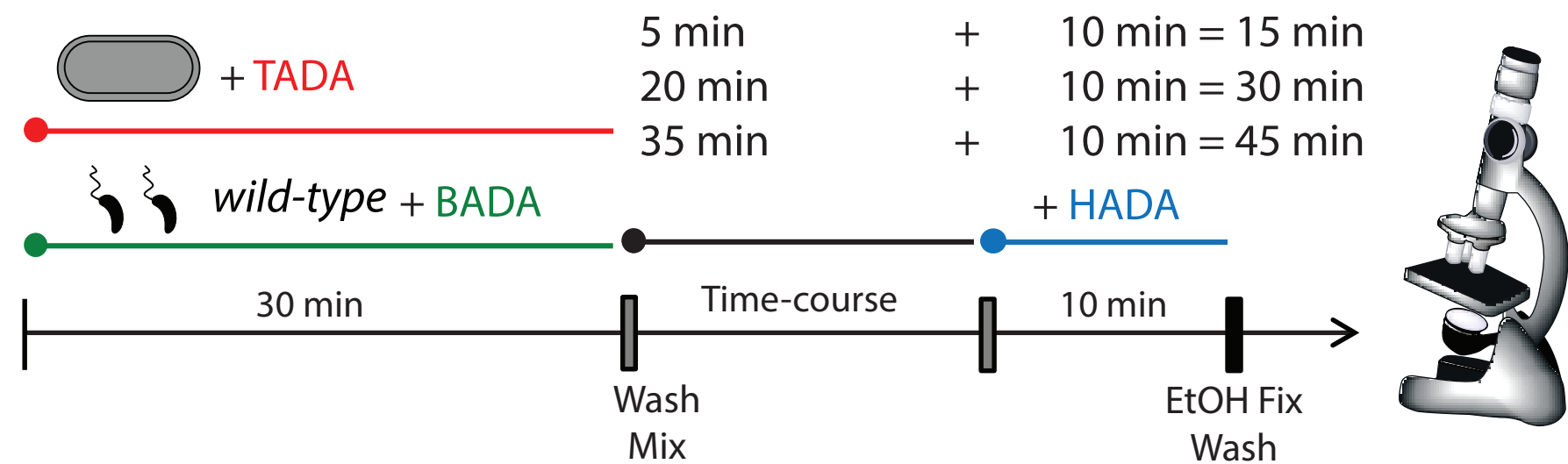
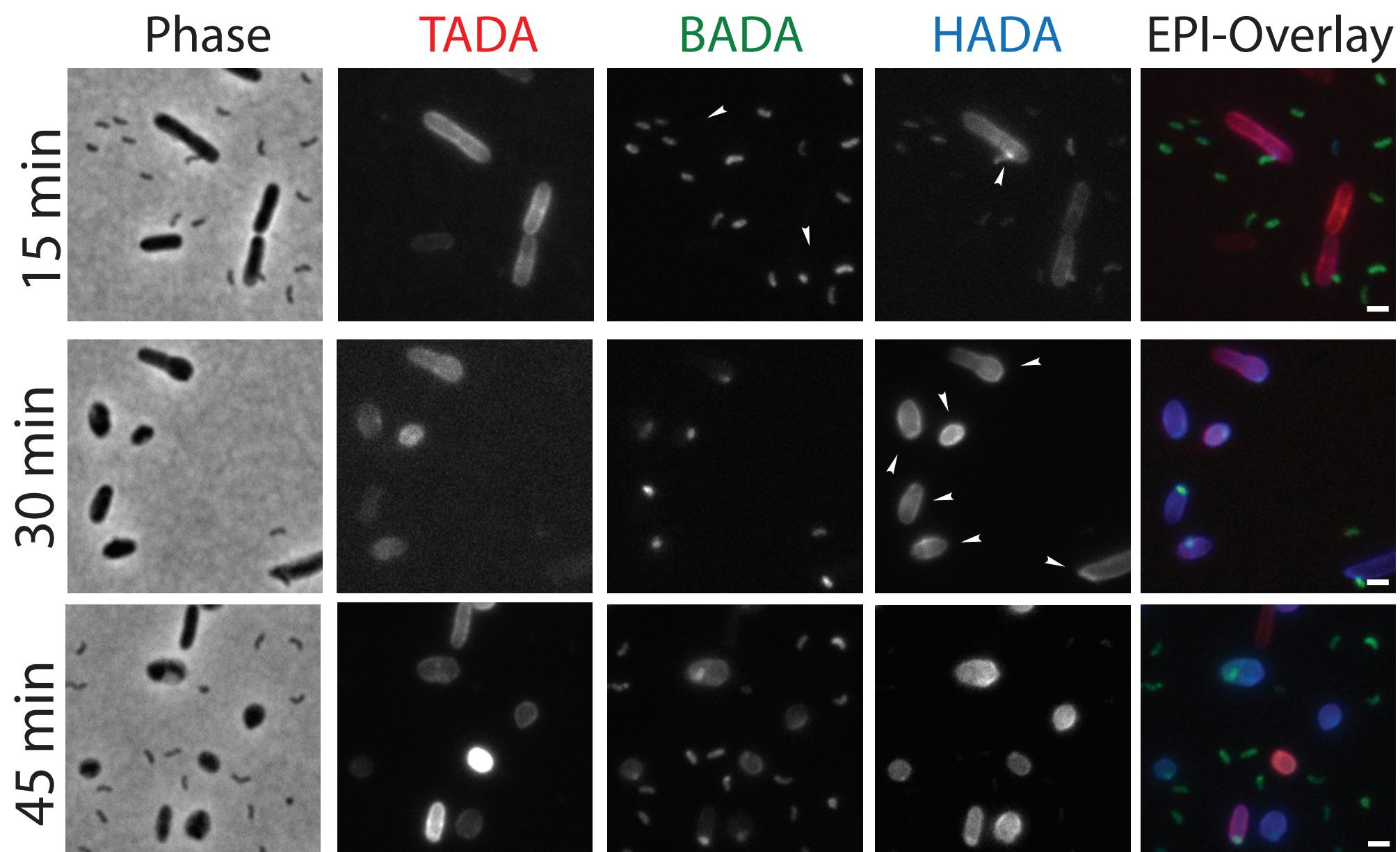
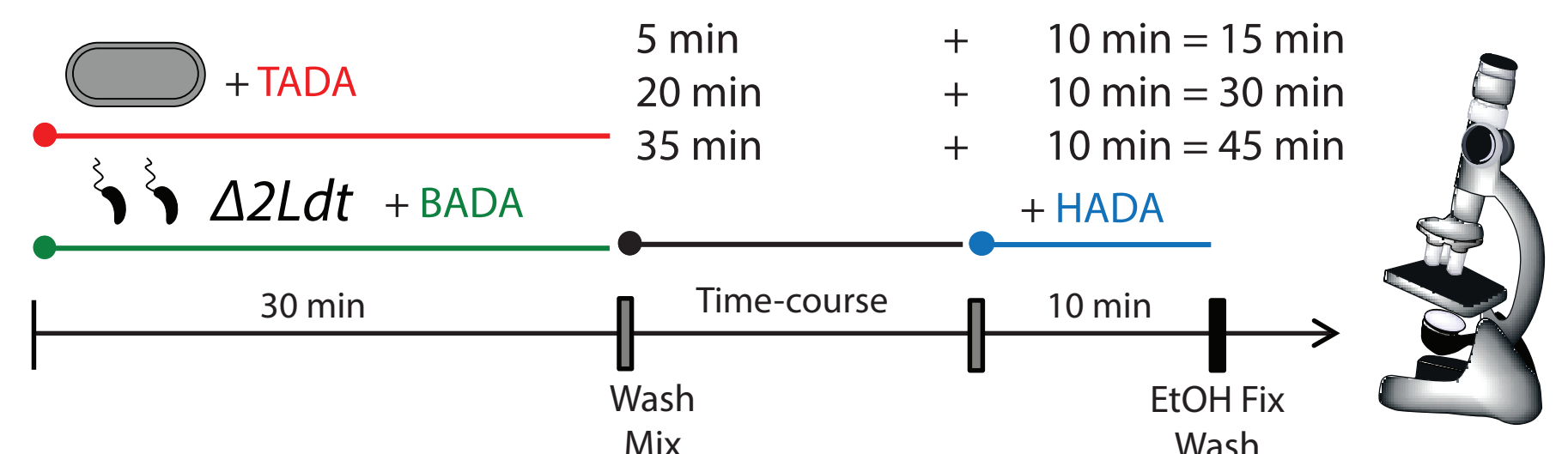
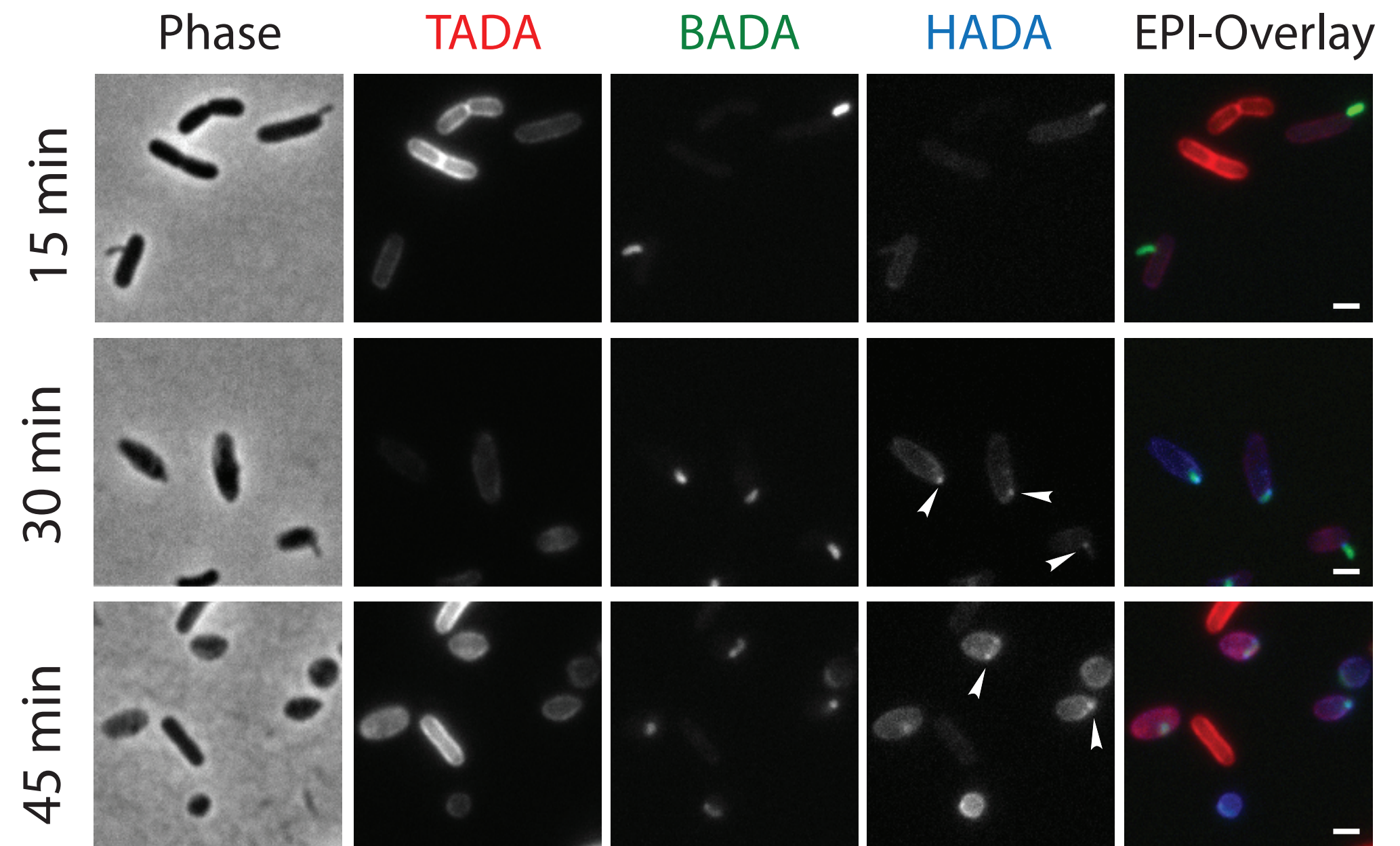
821 44 Datsenko, K. A. & Wanner, B. L. One-step inactivation of chromosomal genes in *Escherichia*
822 *coli* K-12 using PCR products. *Proc Natl Acad Sci U S A* **97**, 6640-6645,
823 doi:10.1073/pnas.120163297 (2000).

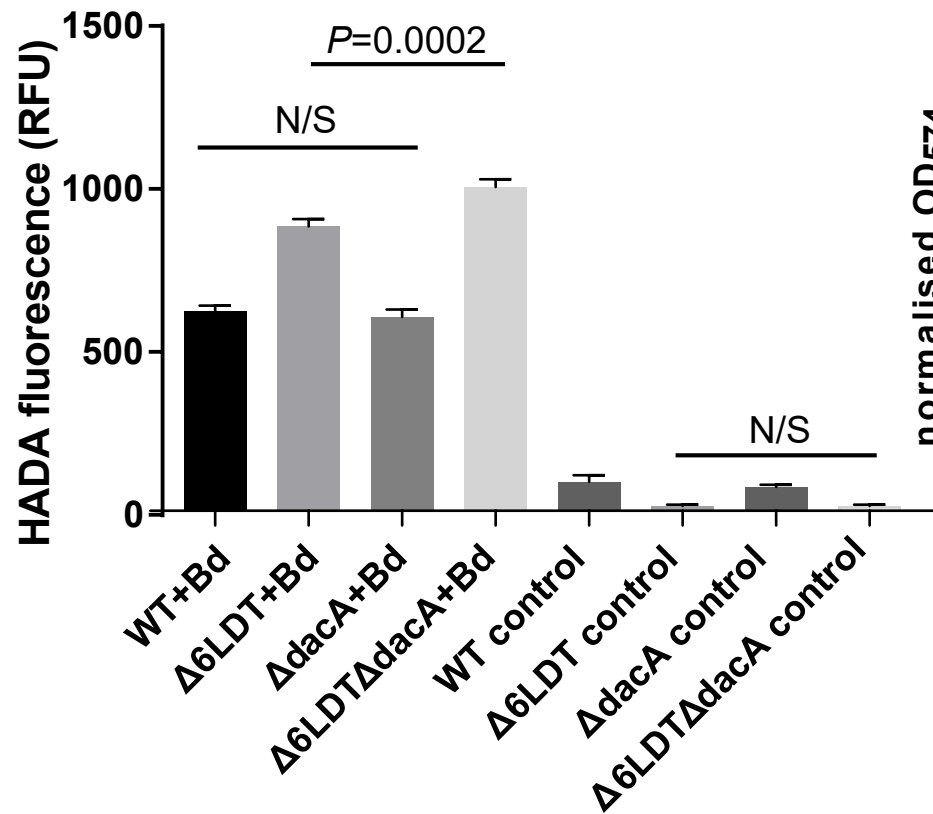
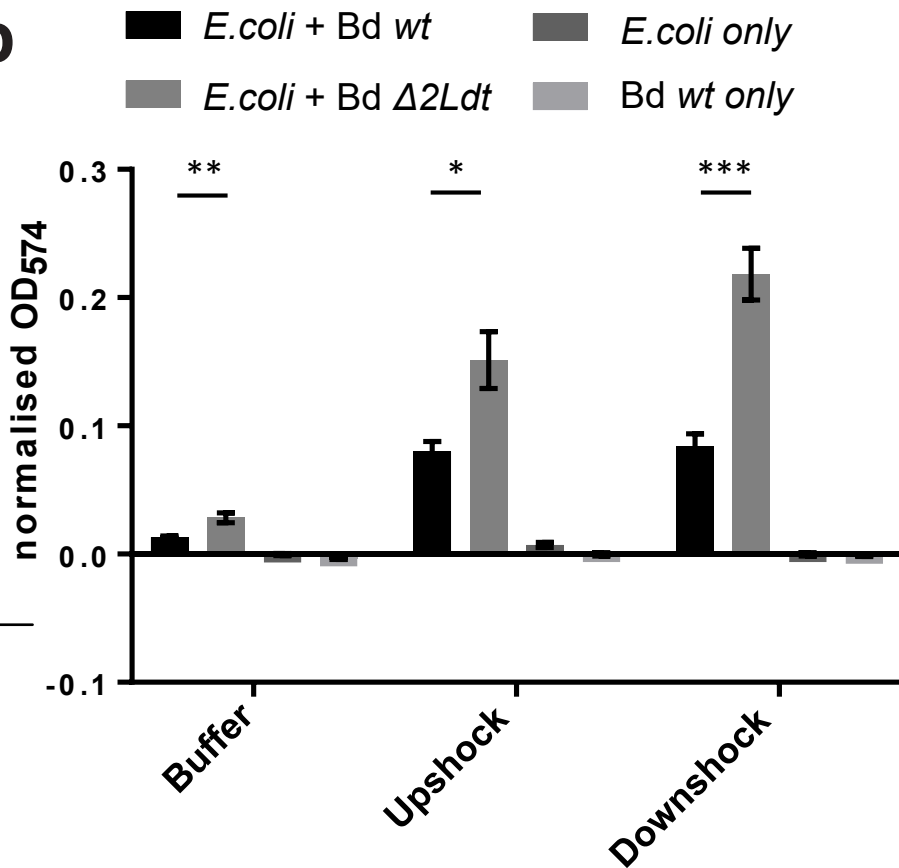
824 45 Fenton, A. K., Lambert, C., Wagstaff, P. C. & Sockett, R. E. Manipulating each MreB of
825 *Bdellovibrio bacteriovorus* gives diverse morphological and predatory phenotypes. *J Bacteriol*
826 **192**, 1299-1311, doi:JB.01157-09 [pii]10.1128/JB.01157-09 (2010).
827 46 Ducret, A., Quardokus, E. M. & Brun, Y. V. MicrobeJ, a tool for high throughput bacterial cell
828 detection and quantitative analysis. *Nature Microbiology* **In press** (2016).
829



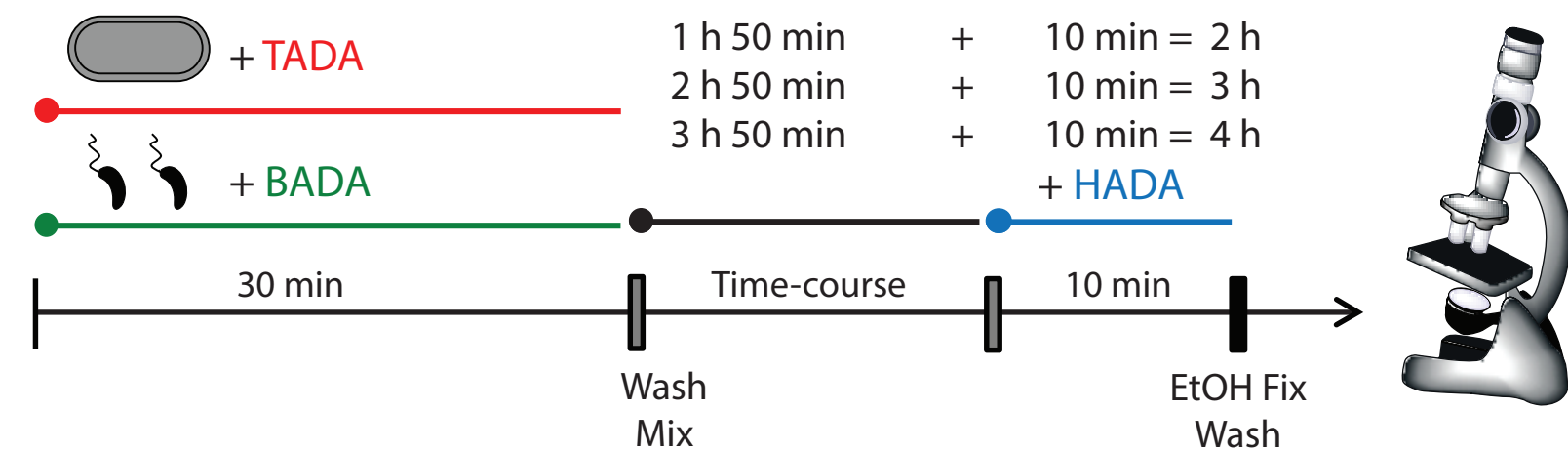
a**BADA****HADA****SIM-Overlay****HADA****SIM-Overlay****SIM-Overlay****b****HADA****BADA****Overlay****c****BADA****HADA****Overlay**

a**TADA****BADA****HADA****SIM-Overlay**
(TADA-HADA)**SIM-Overlay**
(TADA-BADA-HADA)**b****c**

aMean **HADA** signal retained**b****c**Each channel is adjusted individually for **qualitative** comparison**d**Each channel is adjusted individually for **qualitative** comparison

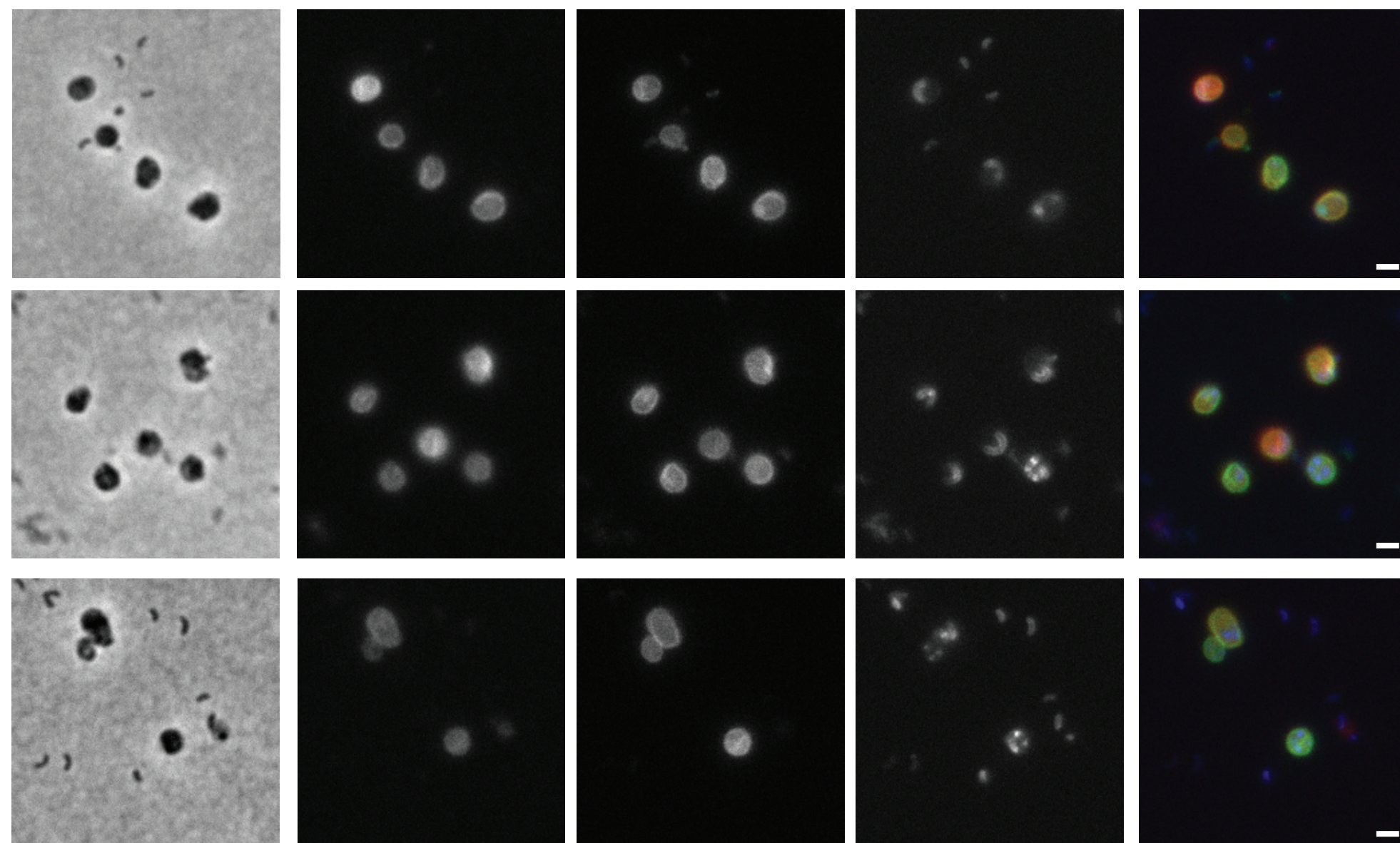
a**b**

a



Each channel is adjusted individually for **qualitative** comparison

Phase TADA BADA HADA EPI-Overlay



TADA

BADA

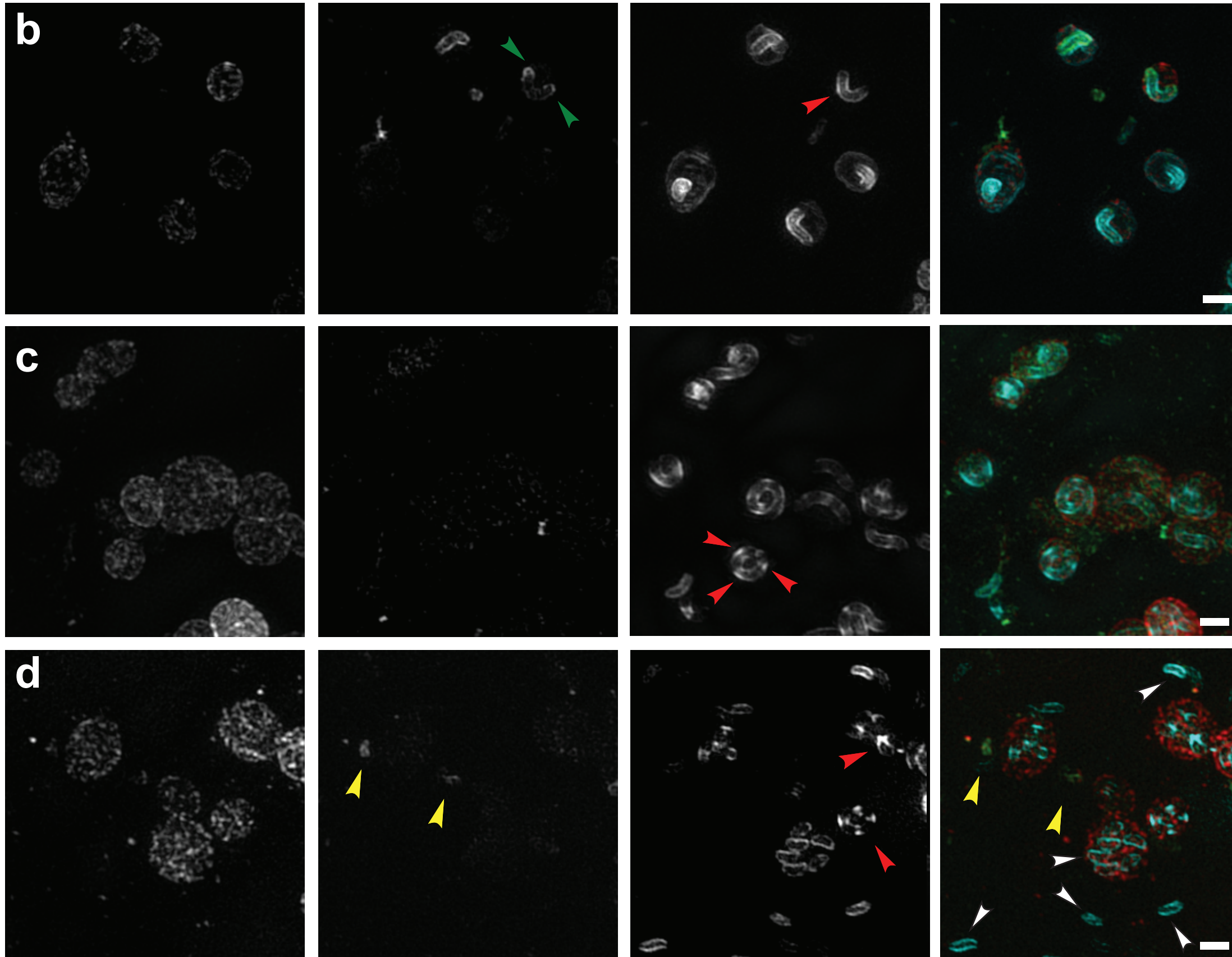
HADA

SIM-Overlay
(TADA-BADA-HADA)

2h

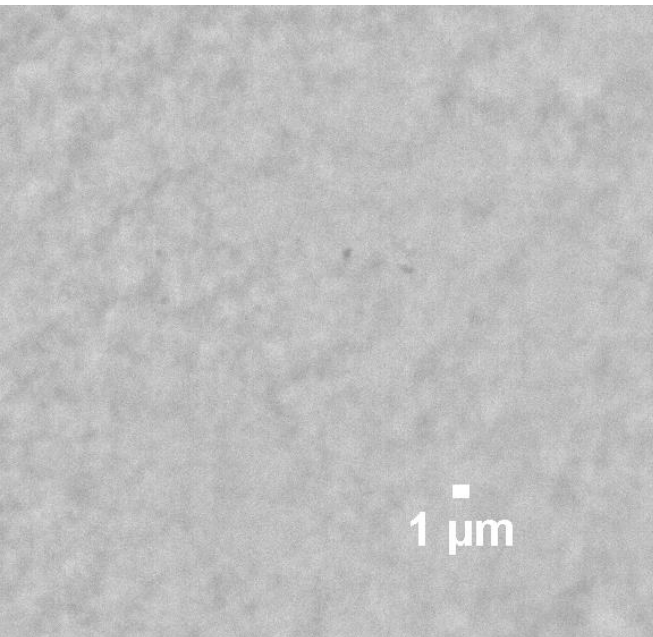
3h

4h

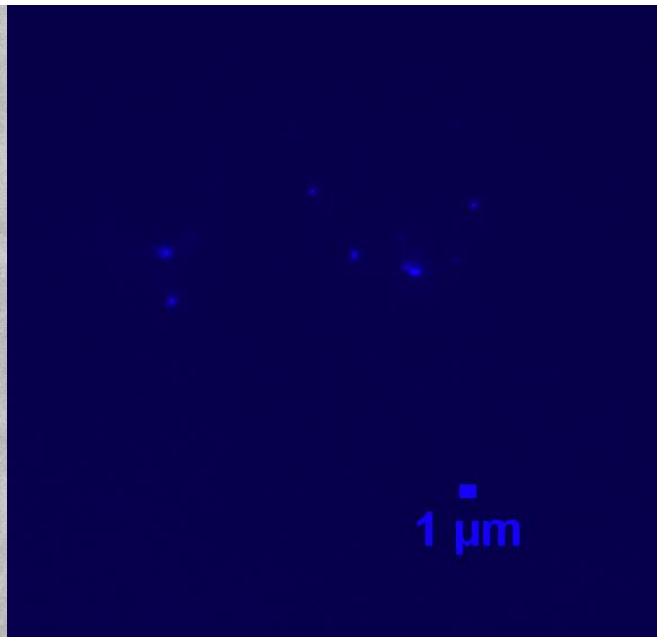


Bdellovibrio sacculi labelled with Br-HADA

Phase

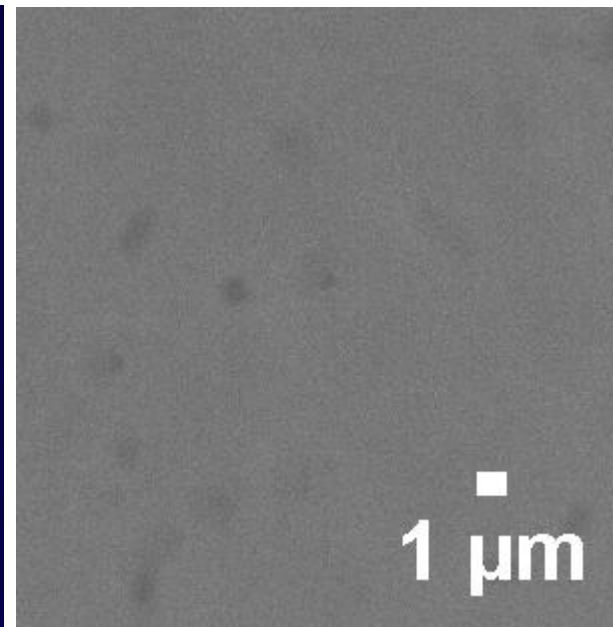


Fluorescence

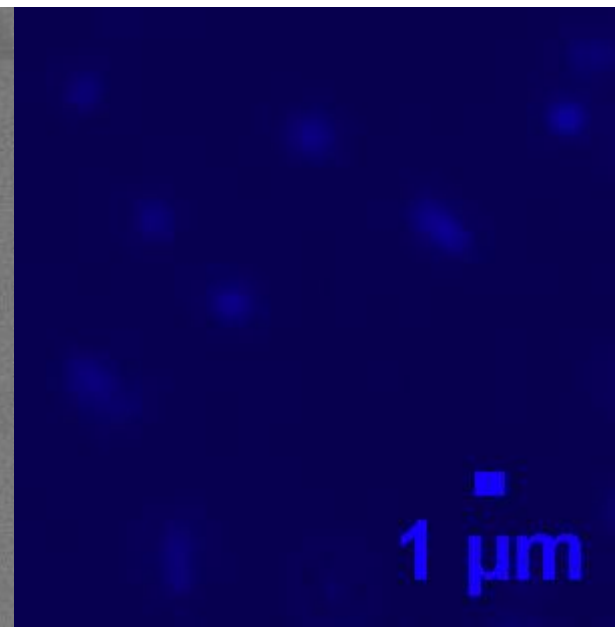


E. coli sacculi labelled with Br-HADA

Phase



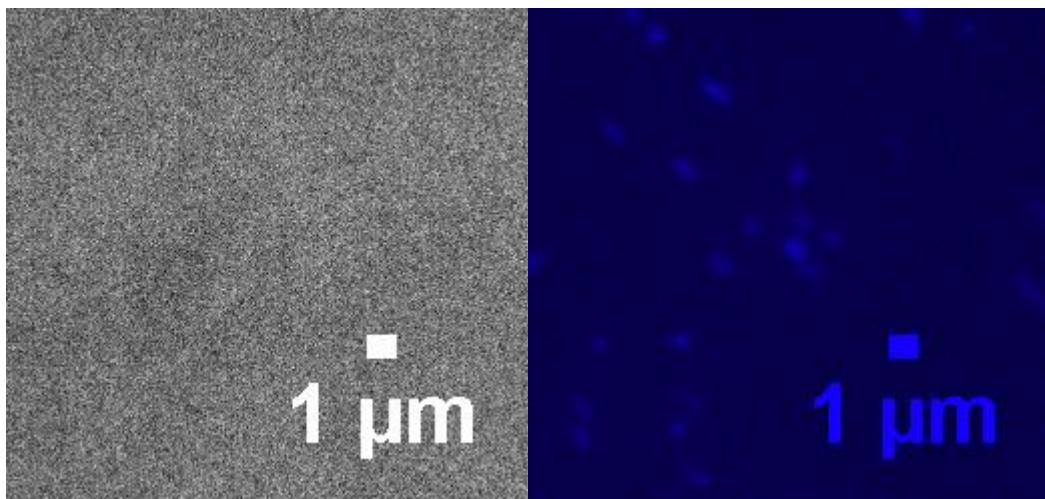
Fluorescence



Bdellovibrio sacculi labelled with HADA

Phase

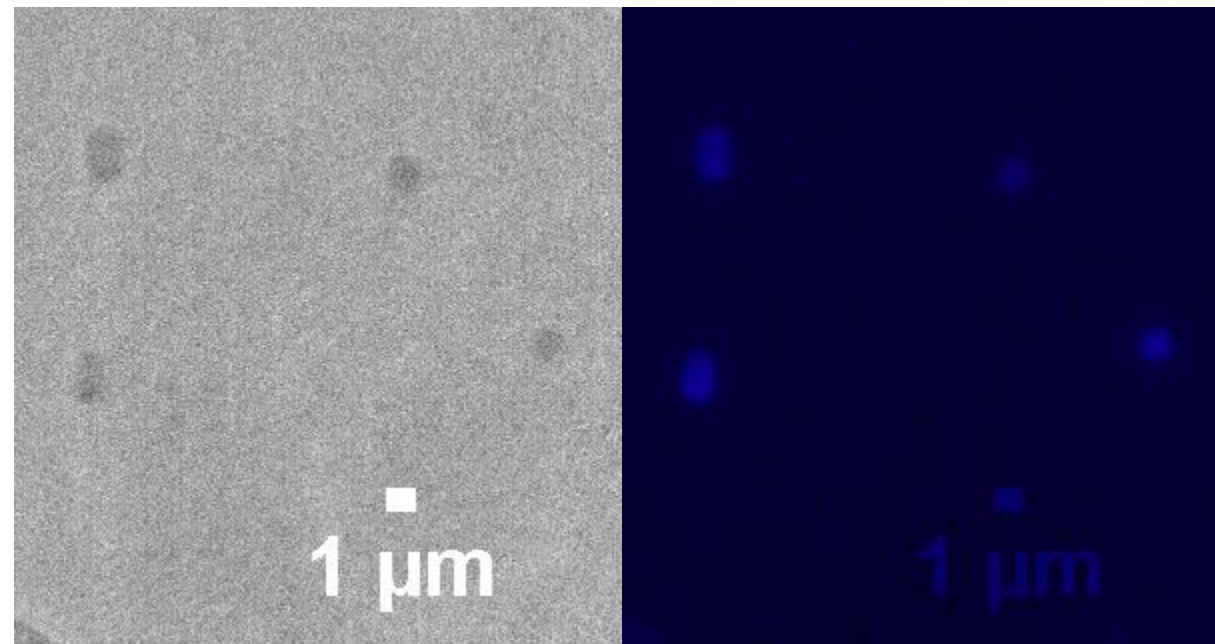
Fluorescence



E. coli sacculi labelled with HADA

Phase

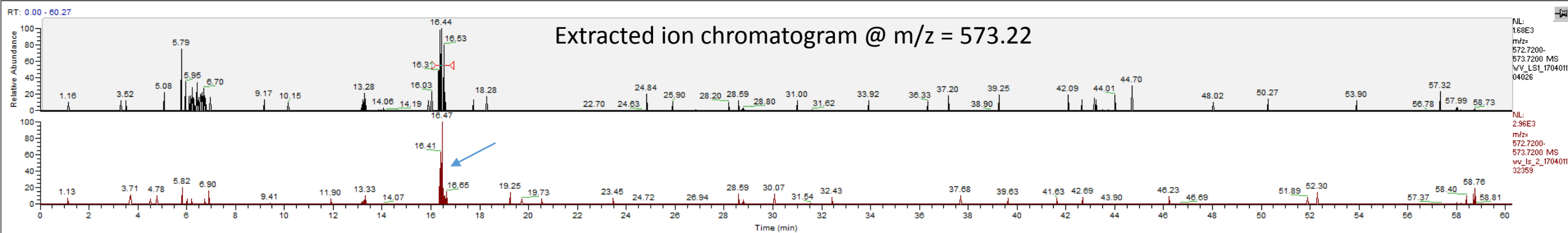
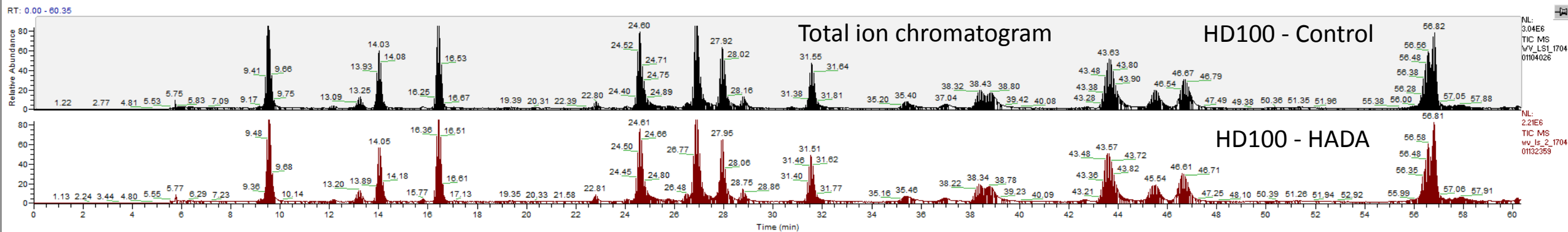
Fluorescence



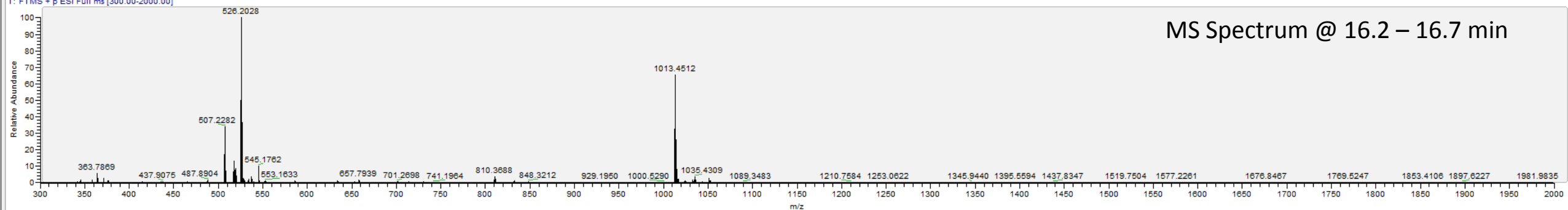
Liz Sockett: Sample 1 / Sample 2 – HD100 – Control / HADA

X:\data\...17_03_31\WV_L1_170401104026

01/04/2017 10:40:26



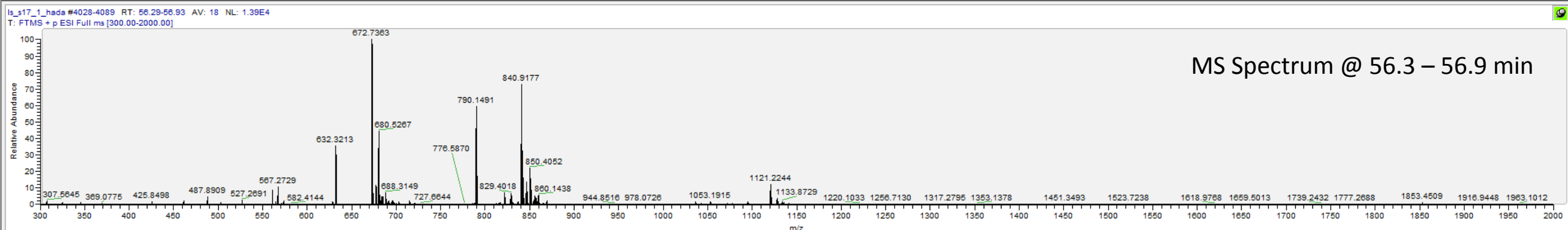
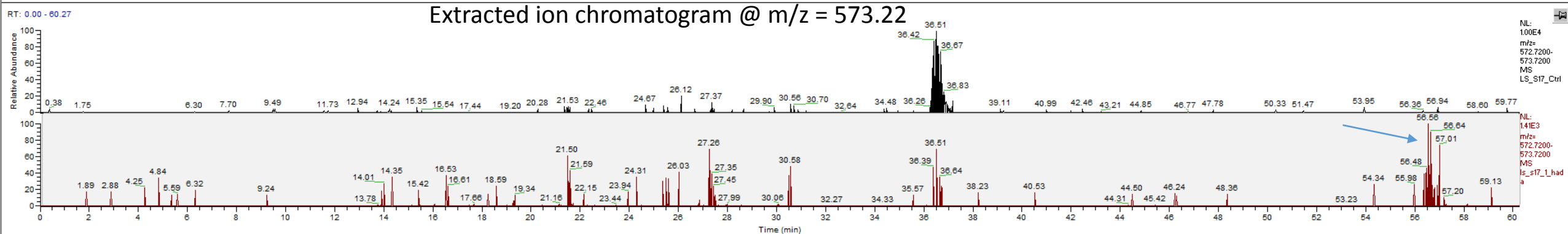
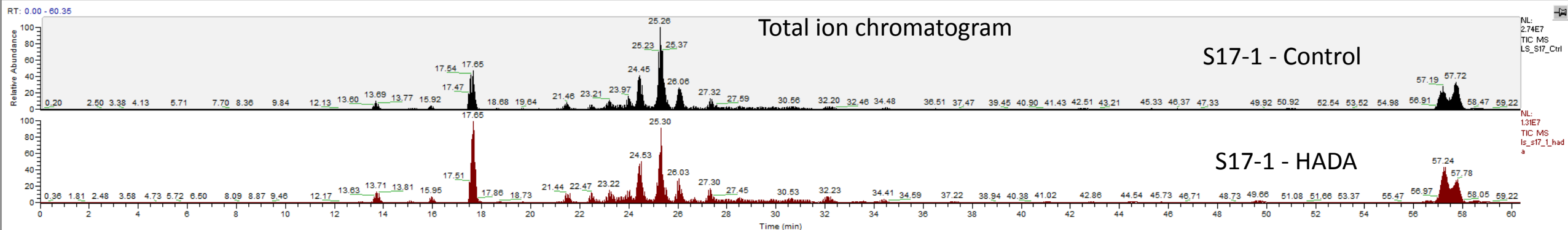
WV_L1_170401104026 #894-961 RT: 16.19-16.74 AV: 14 NL: 1.90E5
T: FTMS + p ESI Full ms [300.00-2000.00]



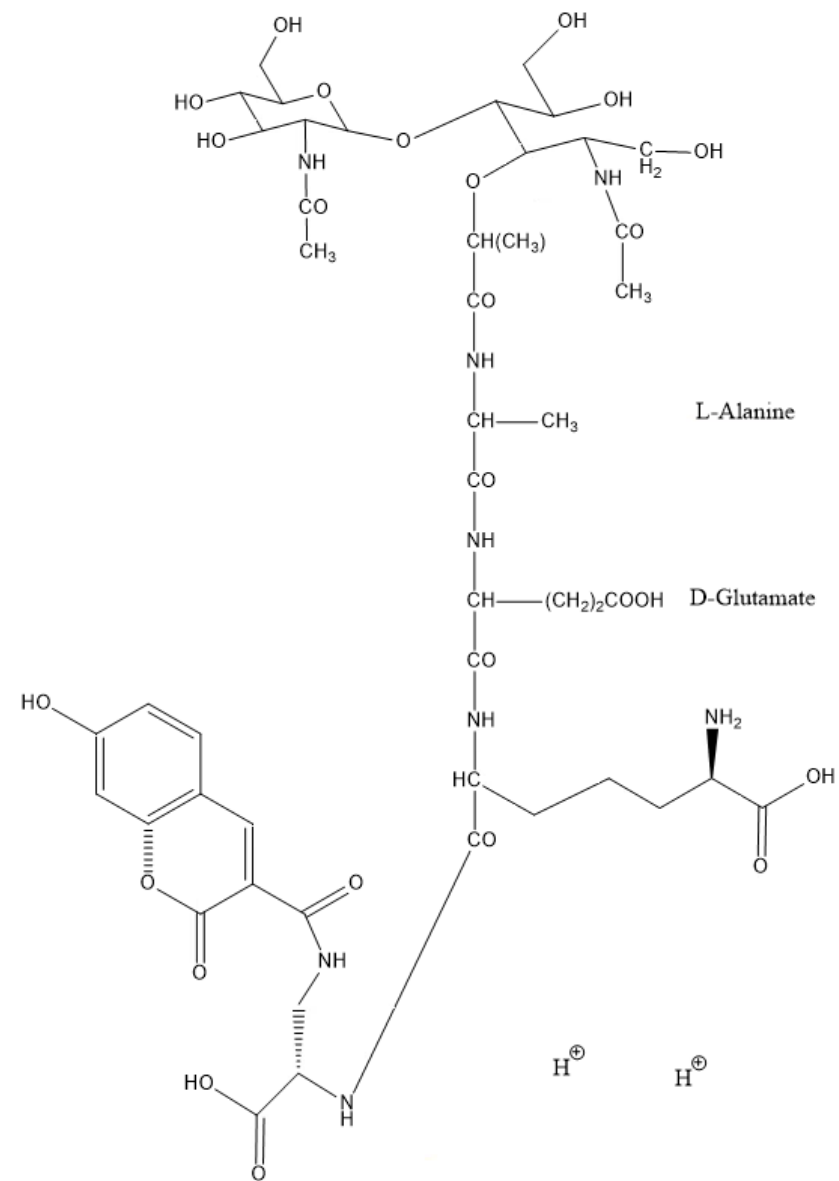
Liz Sockett: Sample 3 / Sample 4 – S17-1 – Control / HADA

x:\data\advance\17_04_12\ls_s17_1_hada

13/04/2017 03:47:56



Liz Sockett: HADA-Labelled MP Product 2= ion @ $m/z = 573.22$



Chemical Formula: $C_{47}H_{70}N_8O_{25}^{2+}$

Exact Mass: 1146.4441

m/z : 573.2221